

Electronic Supplementary Information

Aggregates of Perylene bisimide stabilized superparamagnetic Fe₃O₄ nanoparticles: an efficient catalyst for the preparation of propargylamines and quinolines *via* C-H activation

Sandeep Kaur, Manoj Kumar and Vandana Bhalla*

Department of Chemistry, UGC Sponsored Centre for Advanced Studies-I, Guru Nanak Dev University, Amritsar 143005, and Punjab, India

vanmanan@yahoo.co.in

- S5-S6** General Experimental Procedures.
- S7-13** Synthetic scheme of compounds.
- S14** Comparison of present method over other reported procedure in literature for the preparation of Fe₃O₄ nanoparticles.
- S15** Catalytic application of Fe₃O₄ nanoparticles in three-component Coupling of Aldehydes, Amines, and Alkynes
- S16** Comparison of catalytic activity of Fe₃O₄NPs for formation of aldehydes free propargylamines synthesis over other reported methods.
- S17** Comparison of catalytic activity of Fe₃O₄NPs for formation of quinoline derivatives over other reported methods.
- S18** Absorption spectra and fluorescence spectra of **3** (5 μM) in the presence of different fractions of H₂O/THF mixture.
- S19** UV-vis absorption spectra of derivative **3** upon increasing temperature up to 70⁰C in (H₂O/THF (3:7, v/v).
- S20** Concentration dependent ¹H NMR spectrum of compound **3** and SEM image of derivative **3** in (H₂O/THF (3:7, v/v).
- S21** UV-vis spectra of compound **3** upon additions of various metal ions as their chloride and perchlorate salt in H₂O/THF (3:7, v/v)

- S22** UV-Vis-NIR of compound **3** (5 μM) showing the response to the Fe^{2+} ion (0-35 equiv.) in $\text{H}_2\text{O}/\text{THF}$ (3:7, v/v) mixture and fluorescence excitation spectrum of **3** (5 μM) in addition of Fe^{2+} ions for the emission at 534 nm in $\text{H}_2\text{O}/\text{THF}$ (3:7, v/v) mixture.
- S23** Detection limit of Fe^{2+} by using compound **3** in $\text{H}_2\text{O}/\text{THF}$ (3:7, v/v).
- S24** Competitive and selectivity graph of derivative **3** towards various metal ions as their perchlorate and chloride salt in $\text{H}_2\text{O}/\text{THF}$ (3:7, v/v).
- S25** Time resolved fluorescence decays of **3** in $\text{H}_2\text{O}/\text{THF}$ (3:7, v/v) and in the presence of Fe^{2+} ions. Table showing the radiative, non-radiative decay rate constants.
- S26** TEM images, SAED pattern, HRTEM, XRD pattern and raman spectra of Fe_3O_4 nanoparticles.
- S27** DLS, POM image of aggregates of **3** in $\text{H}_2\text{O}/\text{THF}$ (3:7, v/v) mixture in presence of Fe^{2+} ions and magnetic hysteresis loop of Fe_3O_4 nanorods at room temperature
- S28** Fluorescence emission spectra of derivative **3** (5 μM) upon additions of 35 equiv. of 70 wt% tert-butyl hydroperoxide solution in $\text{H}_2\text{O}/\text{THF}$ (3/7, v/v) mixture.
- S29** UV-Vis-NIR spectra showing the presence of Fe (0) nanoparticle bands.
- S30** ^1H NMR spectra of **3** and Fe_3O_4 nanoparticles of **3** after filtration with THF.
- S31** TEM, DLS analysis of compound **3** (5 μM) showing the size of Fe_3O_4 nanorods at temperature 60°C and UV-vis-NIR spectra of compound **3** (5 μM) on addition of Fe^{2+} ions (0-35 equiv.) in 2:1 ratio in $\text{H}_2\text{O}/\text{THF}$ (3:7, v/v) mixture.
- S32** TEM images, DLS of Fe_3O_4 nanoparticles prepared by using 2:1 mixture of derivative **3** and Fe^{2+} ions and UV-vis spectra of compound **3** (5 μM) at pH (12) solution and in methanol/THF (3:7, v/v) mixture after addition of Fe^{2+} ions.
- S33** TEM of compound **3** (5 μM) showing the size of Fe_3O_4 nanorods at pH (12) and DLS analysis of compound **3** (5 μM) showing the size of Fe_3O_4 nanorods at pH (12) and in Methanol/THF (3:7, V/V).

- S34** UV-vis-NIR spectra of compound **3** (5 μ M) on addition of Fe^{2+} ions (0-35 equiv.) in THF (3:7, v/v) mixture and solvent effect on A^3 -coupling reaction.
- S35** Table showing *in situ* generated Fe_3O_4 nanoparticles catalysed A^3 -coupling reaction of various aldehyde, amines and alkynes to give corresponding products.
- S36** Tentative mechanism of Fe_3O_4 nanoparticles for synthesis of propargylamines and magnetic separation Fe_3O_4 nanoparticles in A^3 coupling reaction.
- S37** Recyclability of the Fe_3O_4 nanoparticles catalyst in A^3 coupling reaction and A^3 coupling reaction of benzaldehyde (**4a**), piperidine (**5a**) and phenylacetylene (**6a**) using various amounts of Fe_3O_4 nanoparticles as catalyst.
- S38** Table showing *in situ* generated Fe_3O_4 nanoparticles catalysed propargylamine synthesis under aldehyde free conditions.
- S39** Recyclability and tentative mechanism of Fe_3O_4 nanoparticles in aldehyde free synthesis of propargylamines.
- S40** Table showing *in situ* generated Fe_3O_4 nanoparticles catalysed quinoline synthesis.
- S41** Recyclability and tentative mechanism of Fe_3O_4 nanoparticles in synthesis of quinolines
- S42** ^1H NMR of (a) propargylamine intermediate generated in preparation of (b) quinoline derivative **11b**
- S43** ^1H NMR of spectrum of derivative **3**.
- S44** ^{13}C NMR of spectrum of derivative **3**.
- S45** ESI-MS spectrum of derivative **3**.
- S46** ^1H NMR of spectrum of derivative **7a** and **7b**.
- S47** ^1H NMR of spectrum of derivative **7c** and **7d**.
- S48** ^1H NMR of spectrum of derivative **7e** and **7f**.

- S49** ^1H NMR of spectrum of derivative **7g** and **7h**.
- S50** ^1H NMR of spectrum of derivative **7i** and **7j**.
- S51** ^1H NMR of spectrum of HPB derivative **4h** and **7k**.
- S52** ^1H NMR of spectrum of derivative **9a** and **9b**.
- S53** ^1H NMR of spectrum of derivative **9c** and **9d**.
- S54** ^1H NMR of spectrum of derivative **9e**.
- S55** ^1H NMR of spectrum of derivative **11a** and **11b**.
- S56** ^1H NMR of spectrum of derivative **11c** and **11d**.
- S57** ^1H NMR of spectrum of derivative **11e**.

General Experimental Procedures:

Materials and reagents: All reagents were purchased from Aldrich and were used without further purification. THF was dried over sodium and benzophenone as an indicator. UV-vis studies were performed in THF, distilled water and HEPES buffer (0.05 M) (pH = 7.05).

Instrumentation: UV-vis spectra were recorded on a SHIMADZU UV-2450 spectrophotometer, with a quartz cuvette (path length, 1 cm). The cell holder was thermostatted at 25°C. The fluorescence spectra were recorded with a SHIMADZU-5301 PC spectrofluorimeter. UV-vis spectra were recorded on Shimadzu UV-2450PC spectrophotometer with a quartz cuvette (path length: 1 cm). The cell holder was thermostatted at 25 °C. The scanning electron microscope (SEM) images were obtained with a field-emission scanning electron microscope (SEM CARL ZEISS SUPRA 55). The TEM images were recorded from Transmission Electron Microscope (TEM) - JEOL 2100F. The FT-IR spectra were recorded with VARIAN 660 IR Spectrometer. The dynamic light scattering (DLS) data were recorded with MALVERN Instruments (Nano-ZS). The Time resolved fluorescence spectra were recorded with a HORIBA Time Resolved Fluorescence Spectrometer. ¹H and ¹³C were recorded on a BRUKER-AVANCE-II FT-NMR-AL 300 MHz and 500 MHz spectrophotometer using CDCl₃ as solvent and tetramethylsilane, SiMe₄ as internal standards. Data are reported as follows: chemical shifts in ppm (s), multiplicity (s = singlet, br = broad signal, d = doublet, t = triplet, m = multiplet), coupling constants *J* (Hz), integration and interpretation. Silica gel 60 (60-120 mesh) was used for column chromatography.

Quantum yield calculations: Fluorescence quantum yield was determined by using optically matching solution of rhodamine B ($\Phi_{fr} = 0.65$ in ethanol) as standard at an excitation wavelength of 530 nm and quantum yield is calculated using the equation:

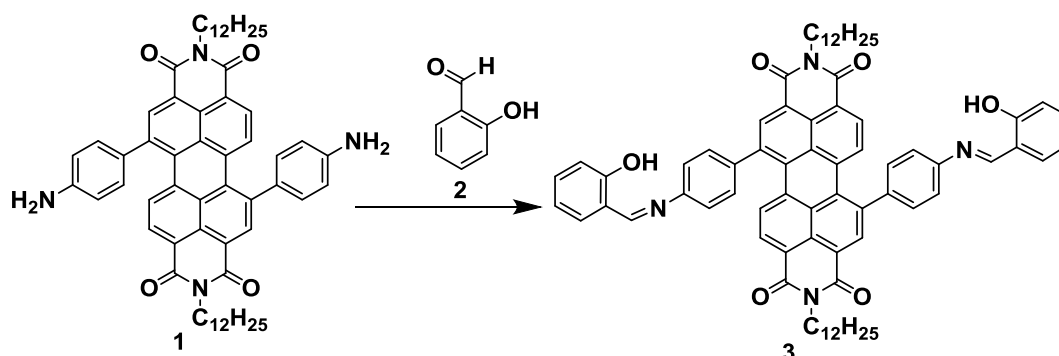
$$\Phi_{fs} = \Phi_{fr} \times \frac{1-10^{-A_r L_r}}{1-10^{-A_s L_s}} \times \frac{N_s^2}{N_r^2} \times \frac{D_s}{D_r}$$

Φ_{fs} and Φ_{fr} are the radiative quantum yields of sample and the reference respectively, A_s and A_r are the absorbance of the sample and the reference respectively, D_s and D_r the respective areas of emission for sample and reference. L_s and L_r are the lengths of the absorption cells of

sample and reference respectively. N_s and N_r are the refractive indices of the sample and reference solutions (pure solvents were assumed respectively).

UV-vis and fluorescence titrations: The concentration of HEPES buffer (pH = 7.05) is 0.05 M. For each experiment we have taken 3 ml solution which contains solution of derivative **3** in 2.1 ml THF and 0.9 ml HEPES buffer (0.05 M, pH = 7.05) or double distilled water. UV-vis and fluorescence titrations were performed with 5.0 μ M solutions of ligand in H₂O/THF (3:7, v/v). Typically, aliquots of freshly prepared standard solutions (10^{-1} M to 10^{-3} M) of metal ions such as Zn²⁺, Hg²⁺, Cu²⁺, Fe²⁺, Fe³⁺, Co²⁺, Pb²⁺, Ni²⁺, Cd²⁺, Ag⁺, Ba²⁺, Al³⁺, Cr³⁺, and Pd²⁺ ions as their perchlorate [M(ClO₄)_x; X = 1-3]/chloride [M(Cl)_x; X = 1-3] in THF/water were added to record the UV-vis and fluorescence spectra.

Synthetic scheme of compound 3:



Scheme 1 Synthesis of PBI based derivative **3**; condition dry THF: MeOH (4:6), 80°C.

Synthesis of compound 3:

A mixture of compound **1** (0.05 g, 0.055 mmol) and salicylaldehyde **2** (12 μ l, 0.011 mmol) in THF-methanol was refluxed for 24 hrs. After the completion of the reaction, the solvent was evaporated and the residue left was crystallized from methanol to give compound **3** in 88% (0.055 g) yield; mp: > 280°C. ^1H NMR (CDCl_3 , 300 MHz): δ = 0.87 [(t, J = 4.5 Hz, 6H, N-CH₂-CH₂-(CH₂)₉-CH₃], 1.19-1.33 [(m, 36H, N-CH₂-CH₂-(CH₂)₉-CH₃], 1.62-1.72 (m, 4H, N-CH₂-CH₂-(CH₂)₉-CH₃), 4.18 (t, 4H, J = 6 Hz, N-CH₂-CH₂-(CH₂)₉-CH₃), 7.02 (d, J = 6 Hz, 2H, ArH), 7.08 (d, J = 9 Hz, 2H, ArH), 7.42-7.50 (m, 8H, ArH), 7.63 (d, J = 9 Hz, 2H, ArH), 7.92 (d, J = 6Hz, 2H, ArH), 8.22 (d, J = 6 Hz, 2H, ArH), 8.65 (s, 2H, ArH), 8.77 (s, 2H, HC=N), 13.13 (s, 2H, OH). ^{13}C NMR (CDCl_3 , 75 MHz): δ = 14.1, 22.7, 27.1, 29.3, 29.4, 29.5, 29.6, 31.9, 35.1, 38.5, 118.5, 120.2, 121.9, 122.1, 123.8, 129.5, 130.7, 133.1, 134.3, 135.8, 137.3, 139.4, 141.9, 153.6, 161.6, 170.8 ppm. ESI-MS mass spectrum of compound **3** showed a parent ion peak, m/z = 1139.5424 [M+Na]⁺. Elemental analysis: Calc. for C, 79.54; H, 6.86; N, 5.01. Found: C, 79.57; H, 6.84; N, 4.99.

Synthesis of Fe₃O₄ Nanoparticles:

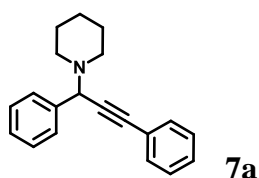
Sample Prepared in 1:1 Ratio: Aqueous solution of 1 M FeCl₂ (450 μ L) was added to a 3 ml solution of compound **3** (0.2 mM) in H₂O/THF (3:7, v/v). The reaction was stirred at room temperature for 270 min and the solution turns brownish-black which indicate the formation of Fe₃O₄ nanoparticles take place. This solution of *in situ* generated nanoparticles was used as such in the catalytic experiment.

Sample Prepared in 2:1 Ratio: Aqueous solution of 1 M FeCl₂ (450 μ L) was added to a 3 ml solution of compound **3** (0.4 mM) in H₂O/THF (3:7, v/v). The reaction was stirred at room

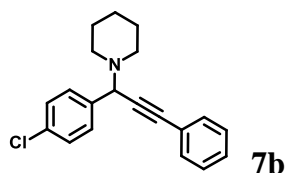
temperature for 180 min and the solution turns brownish-black which indicate the formation of Fe₃O₄ nanoparticles take place. This solution of *in situ* generated nanoparticles was used as such in the catalytic experiment.

General Procedure for the A³-Coupling catalysed by Fe₃O₄ nanoparticles:

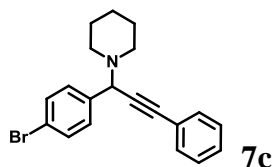
The aldehyde **4a-h** (1.0 mmol), amine **5a-c** (1.2 mmol), and alkyne **6a-b** (1.2 mmol) and Fe₃O₄ catalyst (100/200 μ L, 0.5/1 mol%) were placed in a round-bottom flask in solvent-free conditions at room temperature (except for nitro substitution in toluene at 50°C) and monitored by TLC until total conversion of the starting material. EtOAc (20 mL) was added to the resulting mixture. The crude reaction product was purified by column chromatography (silica gel, hexane/EtOAc), to give the corresponding propargylamines derivatives **7a-k**.



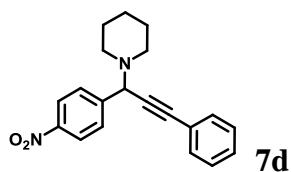
1-(1, 3-diphenylprop-2-ynyl)piperidine (Derivative 7a): ¹H NMR (CDCl₃, 300 MHz): δ = 7.66 (d, J = 9 Hz, 2H), 7.59-7.53(m, 2H), 7.41-7.31(m, 6H), 4.82 (s, 1H), 2.59 (t, J = 4.5 Hz, 4H), 1.64-1.59 (m, 4H), 1.45 (t, J = 12 Hz, 2H).



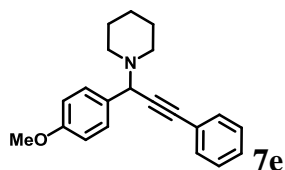
1-(1-(4-Chlorophenyl)-3-phenylprop-2-ynyl)piperidine (Derivative 7b): ¹H NMR (CDCl₃, 300 MHz): δ = 7.58 (d, J = 6 Hz, 2H), 7.55-7.46(m, 2H), 7.34-7.31(m, 5H), 4.76 (s, 1H), 2.53 (t, J = 4.5 Hz, 4H), 1.62-1.54 (m, 4H), 1.47-1.42 (m, 2H).



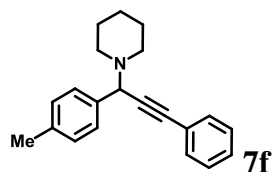
1-(1-(4-Bromophenyl)-3-phenylprop-2-ynyl)piperidine (Derivative 7c): ¹H NMR (CDCl₃, 300 MHz): δ = 7.65-7.59 (m, 2H, ArH), 7.51-7.45 (m, 4H, ArH), 7.39-7.30 (m, 3H, ArH), 4.89 (s, 1H), 2.66 (t, J = 12 Hz, 4H), 1.32-1.25 (m, 4H), 0.89 (t, J = 9 Hz, 2H).



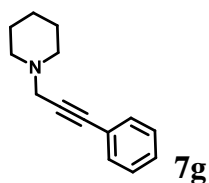
1-(1-(4-Nitrophenyl)-3-phenylprop-2-ynyl)piperidine (Derivative 7d): ^1H NMR (CDCl_3 , 300 MHz): δ = 8.06 (d, J = 6 Hz, 2H, ArH), 7.42 (d, J = 6 Hz, 2H, ArH), 7.28 (t, J = 10.5 Hz, 5H, ArH), 4.65 (s, 1H), 2.49 (t, J = 7.5 Hz, 4H), 1.64-1.51 (m, 4H), 1.32 (t, J = 7.5 Hz, 2H).



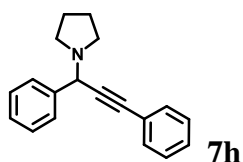
1-(1-(4-Methoxyphenyl)-3-phenylprop-2-ynyl)-piperidine (Compound 7e): ^1H NMR (CDCl_3 , 300 MHz): 7.51-7.49 (m, 4H, ArH), 7.31-7.28 (m, 3H, ArH), 6.89-6.85 (m, 2H, ArH), 4.73 (s, 1H), 3.79 (s, 3H, OMe), 2.60-2.53 (m, 4H), 1.60-1.55 (m, 4H), 1.42 (t, J = 4.5 Hz, 2H).



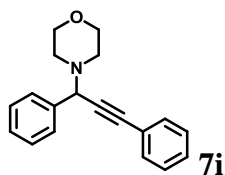
1-(3-phenyl-1-p-tolylprop-2-ynyl)piperidine (Derivative 7f): ^1H NMR (CDCl_3 , 300 MHz): δ = 7.69-7.64 (m, 2H, ArH), 7.58-7.48 (m, 2H, ArH), 7.40-7.35 (m, 3H, ArH), 7.24-7.17 (m, 2H, ArH), 5.08 (s, 1H), 2.82 (t, J = 4.5 Hz, 4H), 2.37 (s, 3H, Me), 1.88-1.74 (m, 4H), 1.58-1.48 (m, 2H).



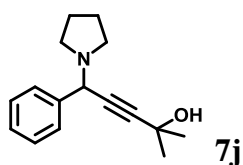
N-(3-Phenyl)prop-2-ynylpiperidine (Derivative 7g): ^1H NMR (CDCl_3 , 300 MHz): δ = 7.34-7.29 (m, 2H, ArH), 7.24-7.17 (m, 3H, ArH), 3.49 (s, 2H), 2.64-2.45 (m, 4H), 1.67-1.57 (m, 4H), 1.46-1.37 (m, 2H).



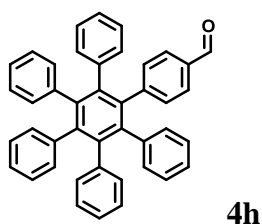
1-(1,3-diphenylprop-2-ynyl)pyrrolidine (Derivative 7h): ^1H NMR (CDCl_3 , 500 MHz): $\delta = 7.47$ (d, 2H, $J = 5$ Hz, 2H, ArH), 7.31-7.27 (m, 5H, ArH), 7.23-7.19 (m, 3H, ArH), 4.95 (s, 1H), 2.42 (t, $J = 7.5$ Hz, 4H), 1.70-1.67 (m, 4H).



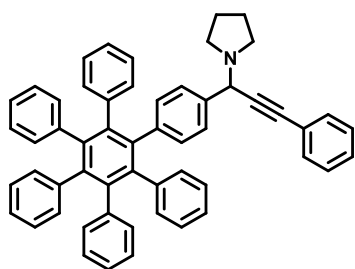
4-(1,3-diphenylprop-2-ynyl)morpholine (Derivative 7i): ^1H NMR (CDCl_3 , 500 MHz): $\delta = 7.51$ (d, 2H, $J = 5$ Hz, 2H, ArH), 7.34-7.27 (m, 5H, ArH), 7.24-7.20 (m, 3H, ArH), 5.23 (s, 1H), 2.42 (t, $J = 5$ Hz, 4H), 2.76-2.72 (m, 4H).



2-Methyl-5-phenyl-5-(pyrrolidin-1-yl)pent-3-yn-2-ol (Derivative 7j): ^1H NMR (CDCl_3 , 500 MHz): $\delta = 7.29$ (d, 2H, $J = 5$ Hz, 4H, ArH), 7.24-7.21 (m, 1H, ArH), 5.33 (brs, 1H, OH), 4.95 (s, 1H), 2.87 (t, $J = 5$ Hz, 4H), 1.70-1.67 (m, 4H), 1.60 (s, 6H).



HPB Derivative 4h: ^1H NMR (CDCl_3 , 300 MHz): $\delta = 9.76$ (s, CHO, 1H), 7.38 (d, $J = 9\text{Hz}$, 2H, ArH), 7.02 (d, $J = 6\text{Hz}$, 2H, ArH), 6.85-6.84 (m, 25H, ArH).

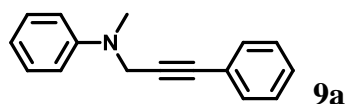


7k

HPB Derivative 7k: ^1H NMR (CDCl_3 , 300 MHz): $\delta = 7.30\text{-}7.25$ (m, 6H, ArH), $7.20\text{-}7.18$ (m, 8H, ArH), $6.86\text{-}6.77$ (m, 20H, ArH), 5.15 (s, 1H), $2.12\text{-}2.01$ (m, 4H), $1.50\text{-}1.44$ (m, 4H).

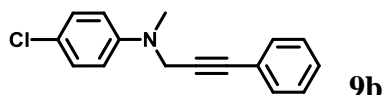
General Procedure for the aldehyde free A^3 -Coupling catalysed by Fe_3O_4 nanoparticles:

In a typical procedure, N,N-dimethylaniline derivative **8a-e** (1.2 mmol), and phenylacetylene **6a** (1.2 mmol) and Fe_3O_4 catalyst (200 μL , 1 mol%) were placed in a round-bottom flask in almost solvent-free conditions at room temperature and monitored by TLC until starting material consumed completely. The reaction mixture was extracted with water/diethyl-ether followed by dried over anhydrous Na_2SO_4 . The crude reaction product was purified by column chromatography (silica gel, hexane/EtOAc), to give the corresponding propargylamines derivatives **9a-e**.



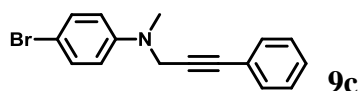
9a

N-Methyl-N-(3-phenylprop-2-ynyl)benzenamine (Derivative 9a): ^1H NMR (CDCl_3 , 500 MHz): $\delta = 7.50$ (d, $J = 5$ Hz, 2H, ArH), $7.33\text{-}7.29$ (m, 1H, ArH), 7.23 (t, $J = 7.5$ Hz, 2H, ArH), 7.09 (t, $J = 7.5$ Hz, 2H, ArH), $6.66\text{-}6.61$ (m, 3H, ArH), 4.45 (s, 2H, N- CH_2), 2.95 (s, 3H, N- CH_3).

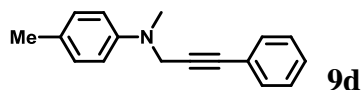


9b

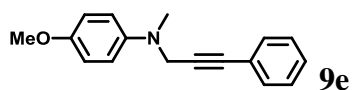
4-Chloro-N-methyl-N-(3-phenylprop-2-ynyl)benzenamine (Derivative 9b): ^1H NMR (CDCl_3 , 500 MHz): $\delta = 7.49$ (d, $J = 10$ Hz, 2H, ArH), 7.30 (t, $J = 7.5$ Hz, 1H, ArH), 7.23 (t, $J = 7.5$ Hz, 2H, ArH), 7.11 (d, $J = 5$ Hz, 2H, ArH), 6.60 (d, $J = 10$ Hz, 2H, ArH), 4.42 (s, 2H, N- CH_2), 2.94 (s, 3H, N- CH_3).



4-Bromo-*N*-methyl-*N*-(3-phenylprop-2-ynyl)benzenamine (Derivative 9c): ^1H NMR (CDCl_3 , 500 MHz): $\delta = 7.50$ (d, $J = 5$ Hz, 2H, ArH), 7.31 (t, $J = 5$ Hz, 1H), 7.27-7.22 (m, $J = 7.5$ Hz, 4H, ArH), 6.50 (d, $J = 5$ Hz, 2H, ArH), 4.42 (s, 2H, N- CH_2), 3.00 (s, 3H, N- CH_3).



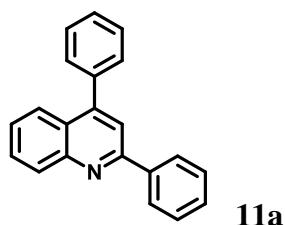
***N*,4-Dimethyl-*N*-(3-phenylprop-2-ynyl)benzenamine (Derivative 9d):** ^1H NMR (CDCl_3 , 500 MHz): $\delta = 7.51$ (d, $J = 6$ Hz, 2H, ArH), 7.32-7.28 (m, 3H), 6.98 (d, $J = 5$ Hz, 2H, ArH), 6.69 (d, $J = 10$ Hz, 2H, ArH), 4.02 (s, 2H, N- CH_2), 2.93 (s, 3H, N- CH_3), 2.36 (s, 3H, CH_3).



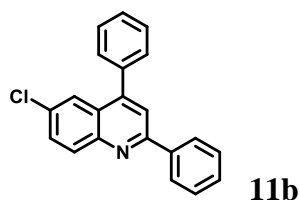
4-Methoxy-*N*-methyl-*N*-(3-phenylprop-2-ynyl)benzenamine (Derivative 9e): ^1H NMR (CDCl_3 , 500 MHz): $\delta = 7.49$ (t, $J = 5$ Hz, 2H, ArH), 7.31-7.29 (m, 3H, ArH), 6.76 (d, $J = 5$ Hz, 2H, ArH), 6.67 (d, $J = 5$ Hz, 2H, ArH), 4.45 (s, 2H, N- CH_2), 3.87 (s, 3H, $-\text{OCH}_3$), 3.00 (s, 3H, N- CH_3).

General Procedure for the synthesis of Quinoline derivatives catalysed by Fe_3O_4 nanoparticles:

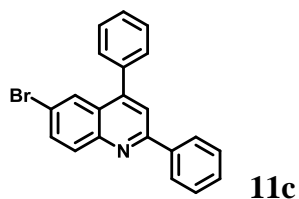
The aldehyde **4a** (1.0 mmol), amine **10a-e** (1.2 mmol), and alkyne **6a** (1.2 mmol) in presence of Fe_3O_4 catalyst (200 μL , 1 mol%) were placed in a round-bottom flask in toluene (10 ml) refluxing at 110 $^\circ\text{C}$ and monitored by TLC until the reactants consumed completely. The resulting reaction mixture was extracted with EtOAc (20 mL) followed by drying over Na_2SO_4 . The crude reaction product was purified by column chromatography (silica gel, hexane/EtOAc), to give the corresponding quinoline derivatives **11a-e**.



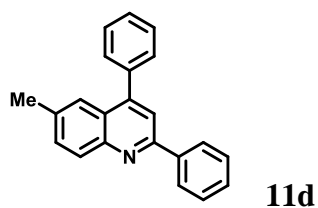
2,4-Diphenylquinoline (Derivative 11a): ^1H NMR (CDCl_3 , 300 MHz): $\delta = 8.54$ (s, 1H, ArH), 8.36-8.29 (m, 2H), 7.98-7.81 (m, 3H), 7.60-7.54 (m, 4H), 7.42-7.34 (m, 5H).



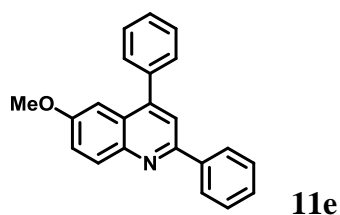
6-Chloro-2,4-diphenylquinoline (Derivative 11b): ^1H NMR (CDCl_3 , 300 MHz): $\delta = 8.15$ (d, $J = 6$ Hz, 3H, ArH), 7.84-7.79 (m, 2H, ArH), 7.60 (s, 1H, ArH), 7.51-7.47 (m, 6H, ArH), 7.16-7.04 (m, 2H).



6-Bromo-2,4-diphenylquinoline (Derivative 11c): ^1H NMR (CDCl_3 , 300 MHz): $\delta = 8.28$ (d, $J = 6$ Hz, 1H, ArH), 8.22-8.14 (m, 2H), 7.91 (s, 1H, ArH), 7.62 (s, 1H, ArH), 7.40-7.32 (m, 9H).



6-Methyl-2,4-diphenylquinoline (Derivative 11d): ^1H NMR (CDCl_3 , 300 MHz): $\delta = 8.20$ -8.14 (m, 3H, ArH), 7.79 (s, 1H), 7.66 (s, 1H, ArH), 7.60-7.49 (m, 9H, ArH), 2.48 (s, 3H, Me).



6-Methoxy-2,4-diphenylquinoline (Derivative 11e): ^1H NMR (CDCl_3 , 300 MHz): $\delta = 8.16$ (s, 3H, ArH), 7.89-7.86 (m, 1H), 7.78-7.72 (m, 2H), 7.57-7.54 (m, 6H), 7.20-7.14 (m, 2H), 3.80 (s, 3H, OMe).

Table S1: Comparison of present method over other reported procedure in literature for the preparation of Fe₃O₄ nanoparticles.

Sr. No.	Publication	Method of formation of Fe ₃ O ₄ nanoparticles	Reagent Used	Reducing/Oxidizing agent Used	Reaction time to prepare Fe ₃ O ₄ nanoparticles	Temp. (°C)	Size	Shape of Fe ₃ O ₄ nanoparticles	Recyclability by magnet after reaction
1	Present manuscript	Wet Chemical Method	Compound 3 in Water/THF and FeCl ₂	No	4.5 h	Room Temperature	30-50 nm (length)	Nanorods	Yes
2	<i>Green Chem.</i> , 2015, 17 , 1610-1617	Solvothermal reaction	FeCl ₃ ·6H ₂ O, ethylene glycol, polyvinylpyrrolidone, NaOAc, Glucose	NaOAc	8 h	200	600 nm	Spherical	Yes
3	<i>J. Am. Chem. Soc.</i> 2015, 137 , 2432-2435	Thermal method followed by centrifugation	Fe(acac) ₃ , 1,2-hexadecanediol, oleic acid, oleylamine, 1,2-hexadecanediol, benzyl ether	-	3 h	200/300	>10 nm	Spherical	Not Done
4	<i>ACS Nano</i> , 2015, 9 , 3969-3977	Chemical coprecipitation method	FeCl ₂ , FeCl ₃ , HCl, NaOH, N ₂ atm	NaOH	30 min	r. t.	30 ± 10 nm	Spherical	Yes
5	<i>ACS Nano</i> , 2015, 4 , 3369-3376	Chemical coprecipitation method	FeCl ₂ , FeCl ₃ , HCl, NH ₄ OH, N ₂ atm	NH ₄ OH	2 h	57	10 nm	Spherical	Not Done
6	<i>ACS Nano</i> , 2015, 3 , 3199-3205	Thermochemical method	FeCl ₃ , oleic acid, 1-octadecene, Acetone, THF	-	30 min	310	8-10 nm	Spherical	Not Done
7	<i>Chem. Commun.</i> , 2015, 51 , 5687-5690	Chemical coprecipitation followed by centrifugation	FeCl ₂ , FeCl ₃ , HCl, NaOH, TMAOH	Yes NaOH and HNO ₃	15 min	95	15 ± 2 nm	Spherical	Not Done
8	<i>Ind. Eng. Chem. Res.</i> , 2015, 54 , 4689-4698	Hydrothermal method	FeCl ₃ ·6H ₂ O, FeSO ₄ ·7H ₂ O, NH ₄ OH, glycerol	NH ₄ OH	6 h	90	10-15 nm	Spherical	Yes
9	<i>Chem. Commun.</i> , 2015, 51 , 5432-5435	Chemical coprecipitation method	Diphenylalanine, FeCl ₂ , FeCl ₃ , KOH, Ar atm.	KOH	-	60		Rod	Not Done
10	<i>Chem. Commun.</i> , 2015, 51 , 5982-5985	Hydrothermal method (Autoclave)	FeCl ₃ ·6H ₂ O, NH ₄ OAc, Sodium Citrate, Ethylene glycol	NH ₄ OAc	18 h	210	100 nm	Spherical	Yes
11	<i>Chem. Commun.</i> , 2015, 51 , 4237-4240	Silica-coated	FeCl ₃ ·6H ₂ O, NaHCO ₃ , vitamin C, Centrifugation	NaHCO ₃	8 h	180	5 nm	Spherical	Not Done
12	<i>Chem. Commun.</i> , 2015, 51 , 7132-7135	Fe ₃ O ₄ NPs–DNA Dendrimers	Fe ₃ O ₄ NPs, PBS buffer, bioconjugation polymer	-	15 min	4	500 nm (with polymer)	Spherical	Not Done
13	<i>ACS Appl. Mater. Interfaces</i> , 2014, 6 , 9890–9896	Hydrothermal method (Autoclave)	FeCl ₃ ·6H ₂ O, sodium acetate, trisodium citrate,	sodium acetate	10 h	200	Nanometer	Spherical	Not Done
14	<i>Nanoscale</i> , 2014, 6 , 2286–2291	electrostatic adsorption and hydrolysis	FeCl ₃ ·6H ₂ O, NaCl, PEG-200F, GO	sodium carbonate	30-120 min	120	10-50 nm	Rod	Not Done

Table S2: Comparison of catalytic activity of Fe₃O₄ nanoparticles for formation of propargylamines from aldehydes, amine and alkyne coupling reaction (A³-coupling) over other reported methods:

Sr. No.	Publication	Catalyst Used	Solvent Used	Catalyst Amount	Nano catalysis	Recyclability	Reaction Time	Temp (in °C)
1	Present Manuscript	Fe ₃ O ₄	Neat ^a -toluene ^b	0.5 ^a -1 ^b mol%	Yes	Yes	3-5 h	r. t. ^a – 50 ^b
2	<i>J. Am. Chem. Soc.</i> , 2015, 2015, 137 , 4650-4653	CuI, Organo-cocatalyst (5 Å MS)	DCM/Toluene	3 mol% CuI, 4 mol% Cocatalyst	No	No	3 -12h	r. t.
3	<i>Green Chem.</i> , 2015, 17 , 2330-2334	Cu(OTf) ₂ /Ph-Pybox	Neat	0.1 mmol	No	Yes	1-2 h	-
4	<i>Nat. Commun.</i> , 2014, 5 , 3884	CuBr, Molecular Sieves	Toluene	20 mmol	No	No	24	40
5	<i>J. Org. Chem.</i> , 2014, 71 ,7311-7320	Pyridine-containing ligand with AgBF ₄ /AgOTf	Water/MeOH/Toluene	3 mol%	No	No	4 - 90	100
6	<i>ACS Sustainable Chem. Eng.</i> , 2014, 2 , 855-859	Eggshell membrane (ESM) supported Au-ESM, Ag-ESM	Toluene	20 mg	Yes	Yes	24	100
7	<i>J. Mater. Chem. A</i> , 2013, 1 , 651-656	Graphene-Fe ₃ O ₄	ACN:THF (1:1)	1-5 mol%	Yes	Yes	24 h	80
8	<i>Appl. Organometal. Chem.</i> , 2013, 27 , 300-306	Heterogeneous MCM-TSCuX	Toluene	3 mol%	Yes	Yes	4-10	80-110
9	<i>Beilstein J. Org. Chem.</i> , 2013, 9 , 180-184	CuI and pyrrolidine	CAN	-	No	No	2h	100
10	<i>Org. Lett.</i> , , 2012, 14 , 1942-1945	CuBr/PPh ₃ , MW	Toluene	30 mol%	No	No	30 min-24h	110
11	<i>J. Org. Chem.</i> , 2012, 77 , 5149-5154	CuI, MW	Toluene	0.3 equiv.	No	No	30 min-21h	100
12	<i>Eur. J. Org. Chem.</i> , 2012, 3093-3104	CuNPs/TiO ₂	THF/Water/EtOH/Neat	0.5 mol-%	Yes	Yes	24h	70

Reaction Conditions: ^a Neat (0.5 mol%) at r.t. for all reactions except for ^b Nitro substituted reaction (entry 4, table S8) require toluene (0.1 mol%) at 50°C.

Table S3: Comparison of catalytic activity of Fe₃O₄ nanoparticles for formation of aldehydes free propargylamines over other reported methods:

Sr. No.	Publication	Catalyst used	Oxidising agent	Solvent Used	Catalyst Amount	Nano catalysis	Recyclability	Reaction Time	Temp (in °C)
1	Present Manuscript	Fe ₃ O ₄	No	Neat	1 mol%	Yes	Yes	3-4.5 h	r. t
2	<i>Catal. Sci. Technol.</i> , 2014, 4 , 4281-4288	CuFe ₂ O ₄	TBHP	Dimethylacetamide	5 mol%	Yes	Yes	3h	140
3	<i>J. Mol. Catal. A: Chem.</i> , 2014, 395 , 300-306	MOF-199	TBHP	Dimethylacetamide	5 mol%	No	Yes	2.5h	120
4	<i>Chem. Commun.</i> , 2009, 5024-5026	FeCl ₂ /Cu Br	TBHP	MeOH	0.10 mol%	No	No	24h	r.t
5	<i>Org. Lett.</i> , 2009, 11 , 1701-1704	FeCl ₂	(t-BuO) ₂	Neat	0.2 mmol	No	No	24h	100

Table S4: Comparison of catalytic activity of Fe₃O₄ nanoparticles for formation of quinoline reaction over other reported methods:

Sr. No.	Publication	Catalyst Used	Solvent Used	Catalyst Amount	Nano Catalysis	Recyclability	Reaction Time	Temp (in °C)
1	Present Manuscript	Fe ₃ O ₄	Toluene	1 mol%	Yes	Yes	3.5-6.5 h	110
2	<i>J. Chin. Chem. Soc. (Weinheim, Ger.)</i> , 2015, 62 , 328-334	Fe ₃ O ₄ @SiO ₂ -imid-PMA	solvent-free conditions	0.02 g	No	Yes	55 min	70
3	<i>RSC Adv.</i> , 2014, 4 , 41753-41762.	Fe ₃ O ₄ @SiO ₂	solvent-free conditions	0.025 g	Yes	Yes	45-160 min	110
4	<i>J. Org. Chem.</i> , 2012, 77 , 501-510	AgNTf ₂ and HOTf	toluene	5 mol%	No	No	24h	80
5	<i>Synlett</i> , 2011, 15 , 2157-2162	Yb(OTf) ₃	[bmim][BF ₄]	10 mol%	No	No	MW irradiation at 80 W, 3min.	80
6	<i>Green Chem.</i> , 2010, 12 , 875-878	K-10	1,2-Dichloroethane	-	No	No	MW irradiation 10 min.	100
7	<i>Chem. Eur. J.</i> , 2009, 15 , 6332-6334	FeCl ₃	toluene	10 mol%	No	No	24h	110
8	<i>Tetrahedron</i> 2011, 67 , 8465-8469	Ytterbium pentafluorobenzoate	Neat	2 mol%	No	No	12h	90
9	<i>Tetrahedron</i> , 2008, 64 , 2755-2761	AuCl ₃ /CuBr	MeOH	5 mol%	No	No	several days	r. t.

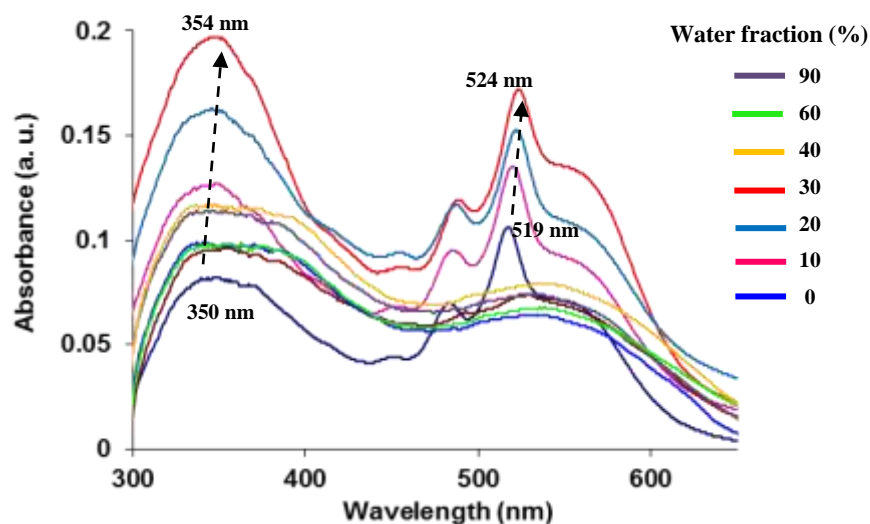


Fig. S1 Absorption spectra of derivative **3** (5 μM) showing the variation of absorption intensity in a $\text{H}_2\text{O}/\text{THF}$ mixture.

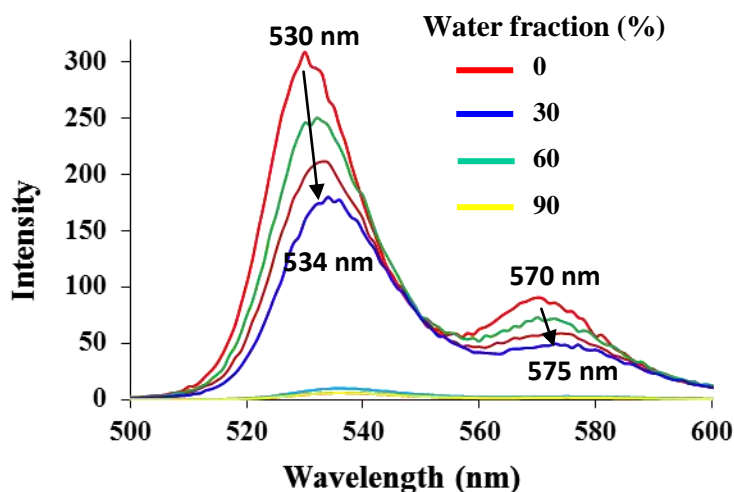


Fig. S2 Fluorescence spectrum of derivative **3** (5 μM) showing the variation of fluorescence intensity in $\text{H}_2\text{O}/\text{THF}$ mixtures; $\lambda_{\text{ex}} = 485 \text{ nm}$.

The UV-vis spectrum of derivative **3** in THF exhibits two absorption bands at 350 and 519 nm. With increasing water fraction upto 30%, both the absorption bands were red shifted ($\sim 5 \text{ nm}$) (Fig. S1). The fluorescence spectrum showed presence of two emission bands at 530 ($\Phi = 0.68$) and 570 nm ($\Phi = 0.55$), however, on increasing water fraction upto 30%, both the bands were red shifted to 534 nm ($\Phi = 0.28$) and 575 nm ($\Phi = 0.25$) respectively, and a decrease in the emission intensity was observed. Further increase in water fraction upto 90% resulted in complete quenching of emission of both the bands. (Fig. S2). The absorbance and emission studies suggest the formation of *J*-aggregates.

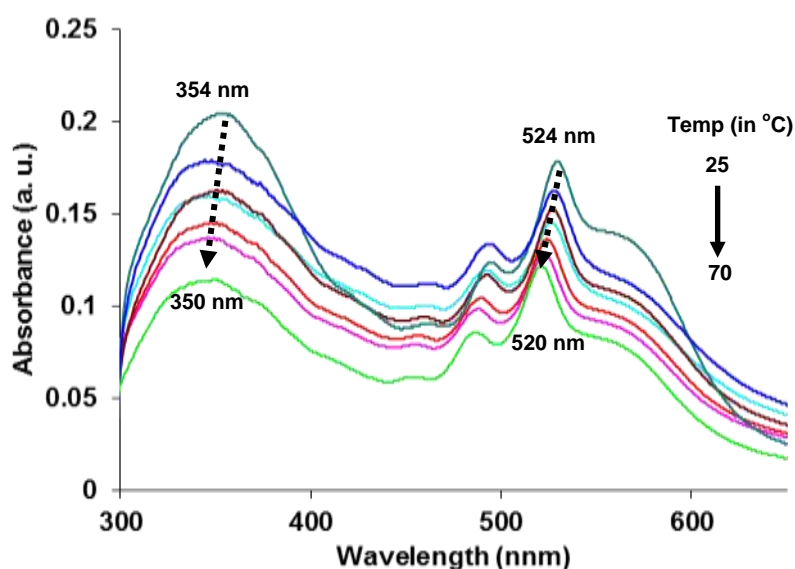


Fig. S3 UV-vis absorption spectra of derivative **3** upon increasing temperature up to 70⁰C in (H₂O/THF (3:7, v/v)).

Temperature dependent UV-vis studies of derivative **3** in H₂O/THF (3:7) was investigated and it was observed that with an increase in temperature up to 70⁰C, the absorption band at 354 and 524 nm were blue shifted to 350 and 520 nm respectively along with gradual decrease in the absorption bands. This study revealed that deaggregation takes place on increasing the temperature, thus, the formation of aggregates of derivative **3** is fully reversible. The above result clearly suggests the deaggregation of *J*-type assemblies on increasing temperature.

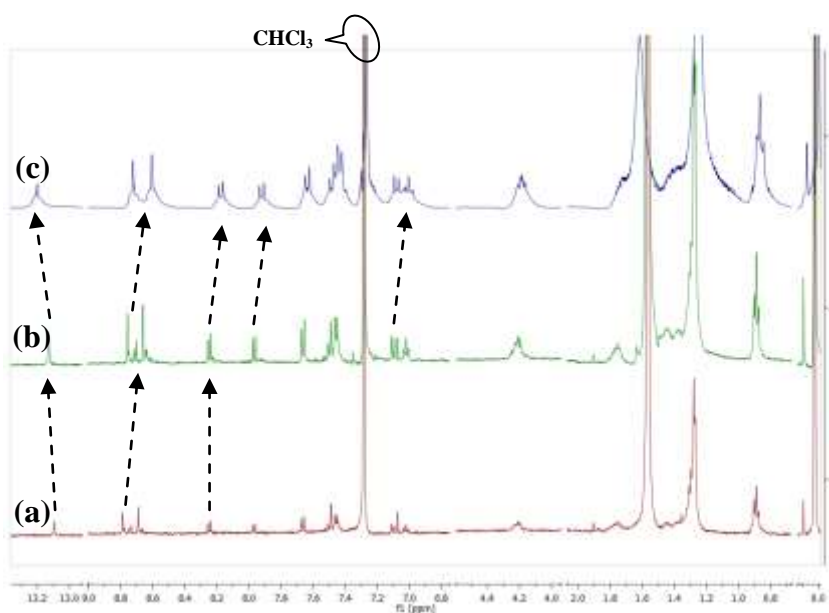


Fig. S4 Concentration dependent ^1H NMR spectrum of compound **3**, (a) 2 mg (b) 5 mg and (c) 10 mg each in 0.6 ml CDCl_3 . NMR frequency is 300 MHz.

Concentration dependent ^1H NMR studies of derivative **3** in CDCl_3 showed the pronounced downfield shift of 0.2 ppm with broadening for the hydroxyl hydrogen atoms along with upfield shifting of 0.08 ppm of the signals corresponding to aromatic protons. These results clearly indicate the molecules are intermolecular hydrogen bonded through the hydroxyl groups as a result of the polymeric nature of the *J*-aggregates.

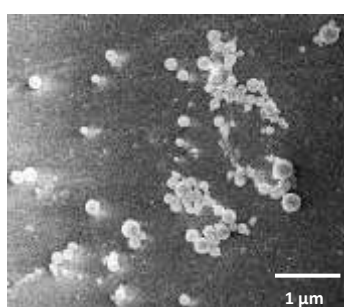


Fig. S5 SEM images of derivative **3** showing the formation of aggregates ($\text{H}_2\text{O}/\text{THF}$ (3:7, v/v)). Scale bar 1 μm

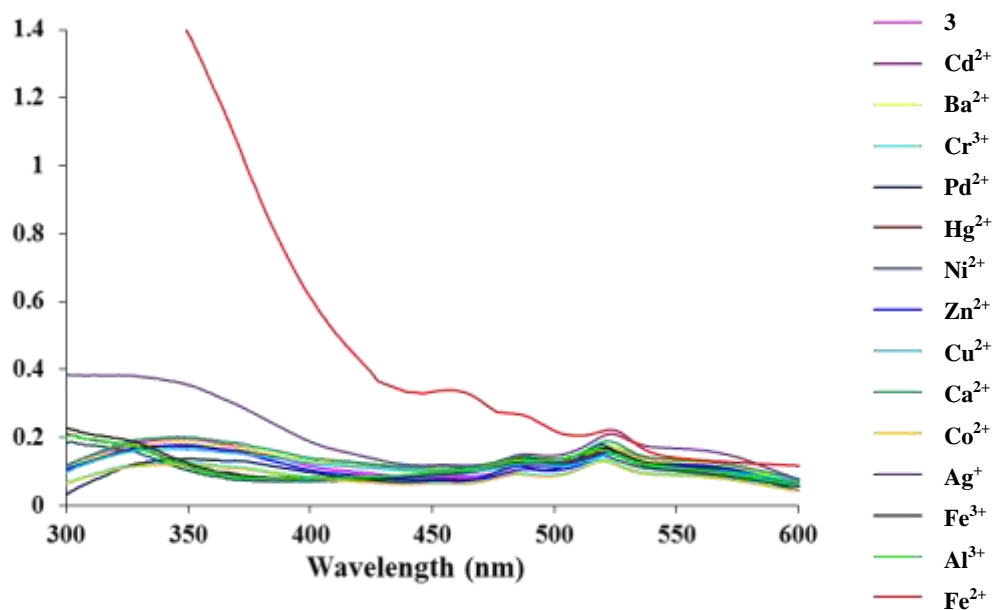


Fig. S6A UV-vis spectra of derivative **3** (5 μM) upon additions of 35 equiv. of various metal ions as their chloride salt in H₂O/THF (3:7, v/v) mixture.

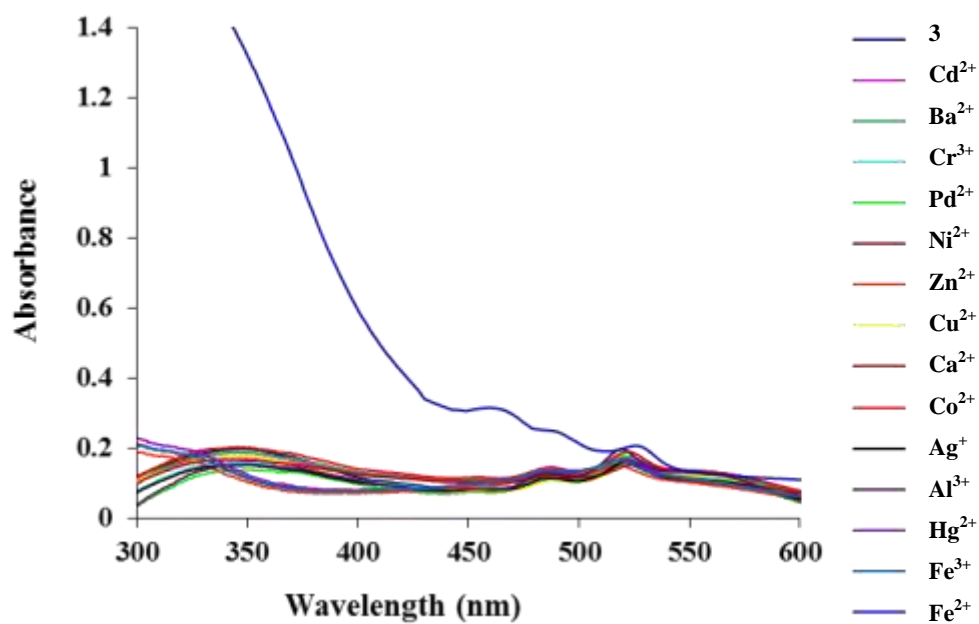


Fig. S6B UV-vis spectra of derivative **3** (5 μM) upon additions of 35 equiv. of various metal ions as their perchlorate salt in H₂O/THF (3:7, v/v) mixture.

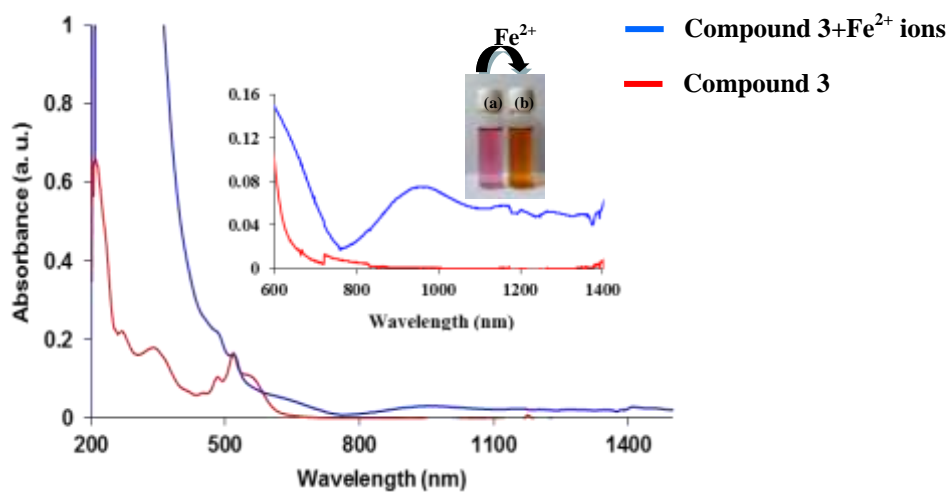


Fig. S7 UV-Vis-NIR spectra of compound **3** (5 μ M) showing the response to the Fe²⁺ ion (0-35 equiv.) in H₂O/THF (3:7, v/v) mixture. Inset photographs (a) before and (b) after the addition of Fe²⁺ ion.

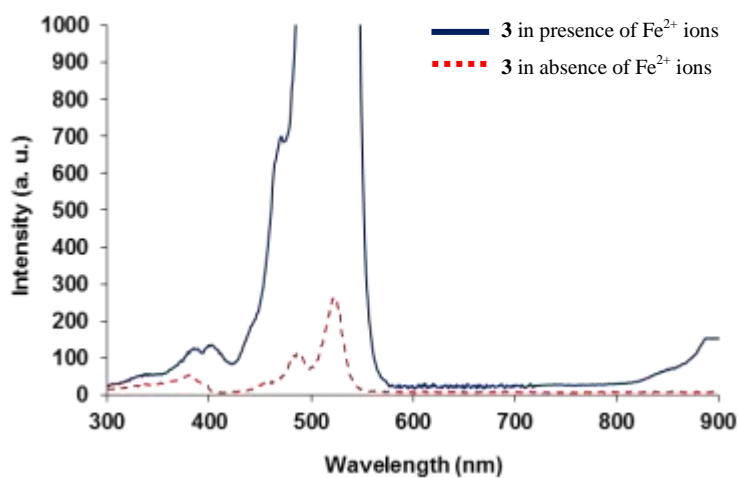


Fig. S8 Fluorescence excitation spectrum of **3** (5 μ M) in H₂O/THF (3:7, v/v) mixture before and after the addition of Fe²⁺ ions for the emission at 534 nm ($\lambda_{em} = 534$ nm).

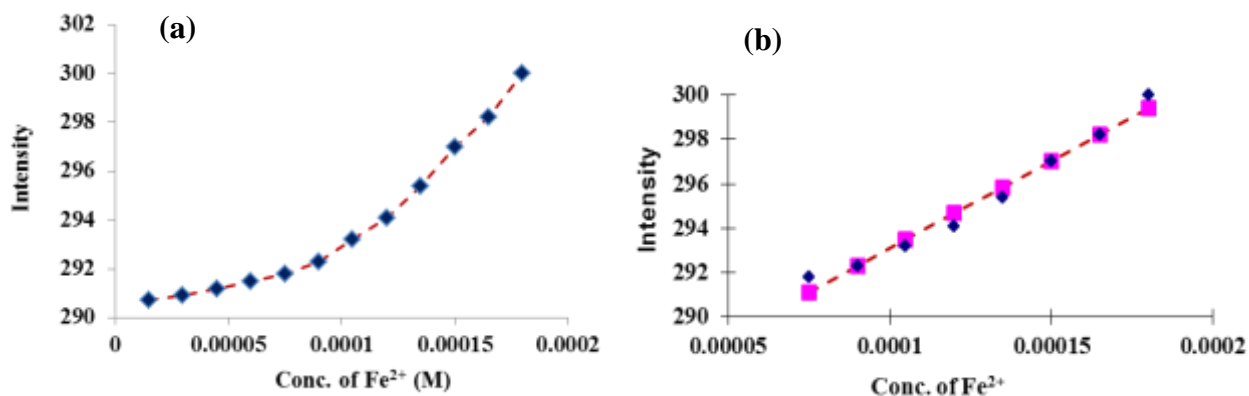


Fig. S9 (a) Showing the fluorescence intensity of compound **3** and (b) Calibrated curve showing the fluorescence intensity of compound **3** at 534 nm as a function of Fe²⁺ ions concentration (equiv.) in H₂O/THF (3:7, v/v) buffered with HEPES, pH =7.05, λ_{ex} = 485nm.

Multiple R = 0.993672,
 $R^2 = 0.987383$,
 Standard deviation = 0.008,
 Observation = 10,
 Intercept = 284.17,
 Slope = 85714.29

The detection limit was calculated based on the fluorescence titration. To determine the S/N ratio, the emission intensity of receptor **3** without Fe²⁺ was measured by 10 times and the standard deviation of blank measurements was determined. The detection limit is then calculated with the following equation:

$$DL = 3 \times SD/S$$

Where SD is the standard deviation of the blank solution measured by 10 times; S is the slope of the calibration curve.

From the graph we get slope

S = **85714.29**, and SD value is 0.008

Thus using the formula we get the Detection Limit (DL) = $3 \times 0.008/85714.29 = 28 \times 10^{-8} \text{ M} = 280 \text{ nM}$

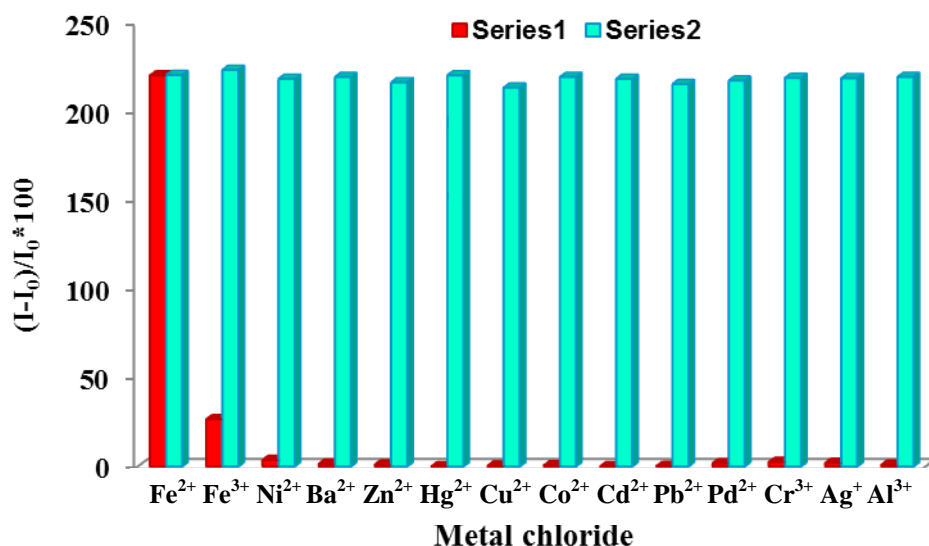


Fig. S10A Fluorescence response of **3** (5.0 μM) to various metal ions of **chloride salts** (70 equiv.) in $\text{H}_2\text{O}/\text{THF}$ (3:7, v/v) mixture buffered with HEPES; $\text{pH} = 7.05$; $\lambda_{\text{ex}} = 485$ nm. Bars represent the emission intensity ratio $(I-I_0)/I_0 \times 100$ (I_0 and I are the initial and final fluorescence intensity at 534 nm before and after the addition of metal ions). (Series 1) Red bars represent selectivity of **3** upon addition of different metal ions. (Series 2) Sky blue bars represent competitive selectivity of receptor **3** toward Fe^{2+} ions (35 equiv.) in the presence of other metal ions (70 equiv.).

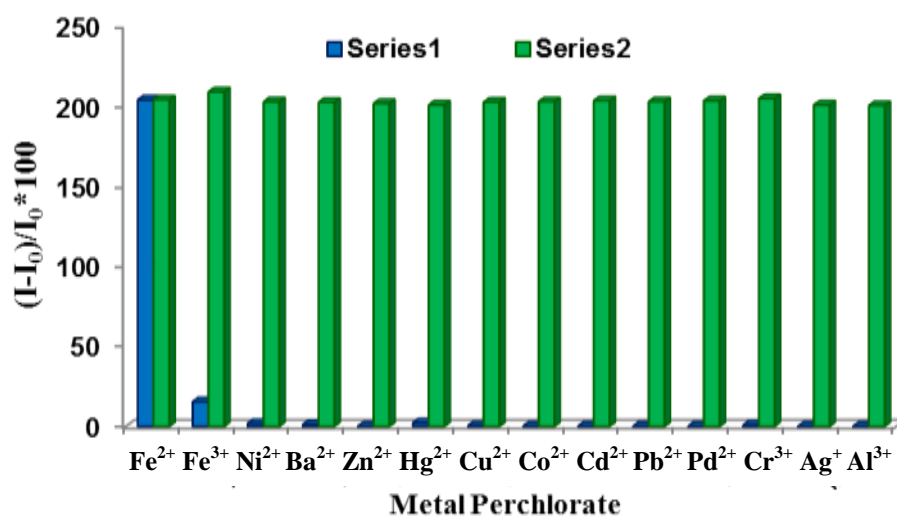


Fig. S10B Fluorescence response of **3** (5.0 μM) to various metal ions of **perchlorate salts** (70 equiv.) in $\text{H}_2\text{O}/\text{THF}$ (3:7, v/v) mixture buffered with HEPES; $\text{pH} = 7.05$; $\lambda_{\text{ex}} = 485$ nm. Bars represent the emission intensity ratio $(I-I_0)/I_0 \times 100$ (I_0 and I are the initial and final fluorescence intensity at 534 nm before and after the addition of metal ions). (Series 1) Blue bars represent selectivity of **3** upon addition of different metal ions. (Series 2) Green bars represent competitive selectivity of receptor **3** toward Fe^{2+} ions (35 equiv.) in the presence of other metal ions (70 equiv.).

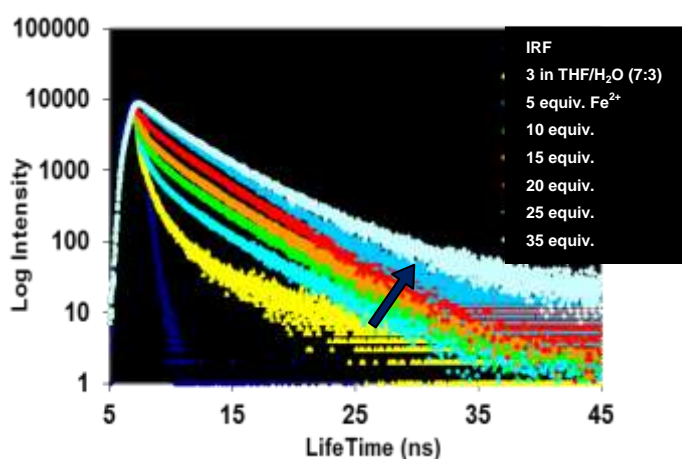


Fig. S11 Exponential fluorescence decays of **3** on addition of Fe^{2+} ions measured at 534 nm. Spectra were acquired in $\text{H}_2\text{O}/\text{THF}$ (3:7, v/v) mixture buffered with HEPES; pH = 7.05; $\lambda_{\text{ex}} = 486 \text{ nm}$

Entry	Quantum Yield	$A_1/A_2/A_3$	Life time (ns)				k_f (10^9 S^{-1})	k_{nr} (10^9 S^{-1})
			τ_1	τ_2	τ_3	τ_{avg}		
Compound 3 (7:3, THF: Water)	0.55	67/33	0.26	2.38	-	0.76	0.723	0.59
Compound 3 + Fe^{2+} (35 equiv.)	0.85	0.15/0.43/9 9.42	2.11	3.51	5.9	5.6	0.151	0.026

Table S5 Fluorescence lifetime of derivative **3** in $\text{H}_2\text{O}/\text{THF}$ (3:7, v/v) and in the presence of Fe^{2+} ions for the emission at 534 nm. A_1, A_2 : fractional amount of molecules in each environment. τ_1, τ_2, τ_3 and τ_{avg} : tri-exponential and average life time of aggregates in 30 vol% of water in THF; k_f : radiative rate constant ($k_f = \Phi_f/\tau_{avg}$); k_{nr} : non-radiative rate constant ($k_{nr} = (1 - \Phi_f)/\tau_{avg}$); $\lambda_{\text{ex}} = 486 \text{ nm}$.

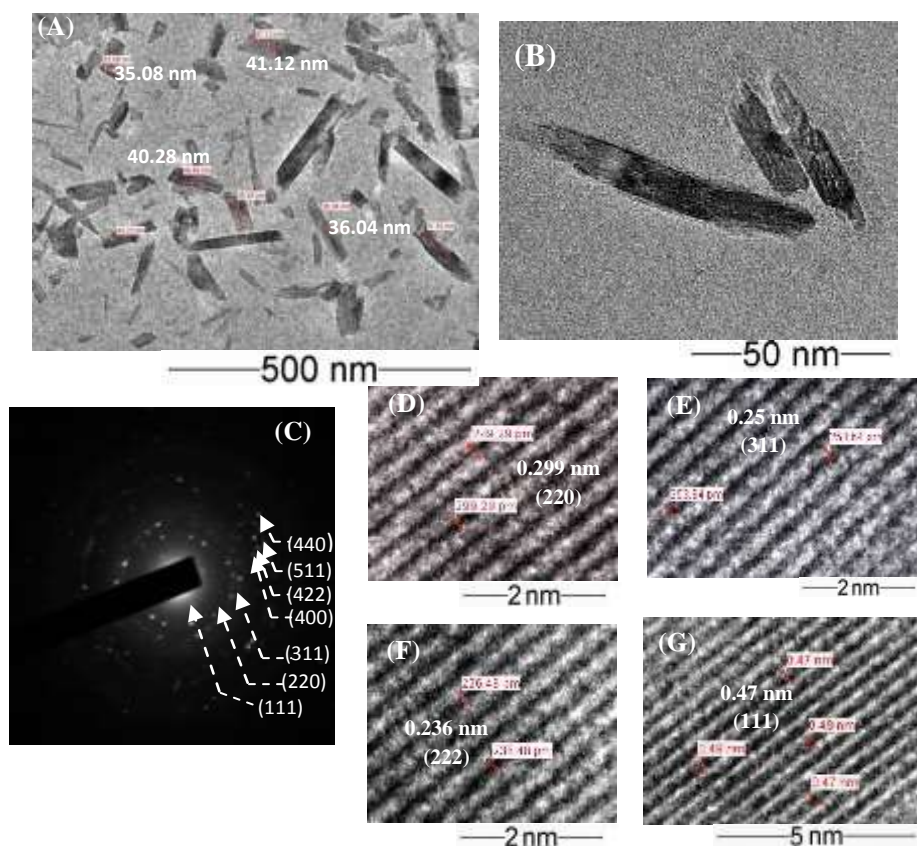


Fig. S12 TEM images of Fe_3O_4 NPs: (A) Scale bar 500 nm, (B) Scale bar 50 nm, (C) SAED pattern from the single nanorod and (D-G) HRTEM images showing the interplanar spacing.

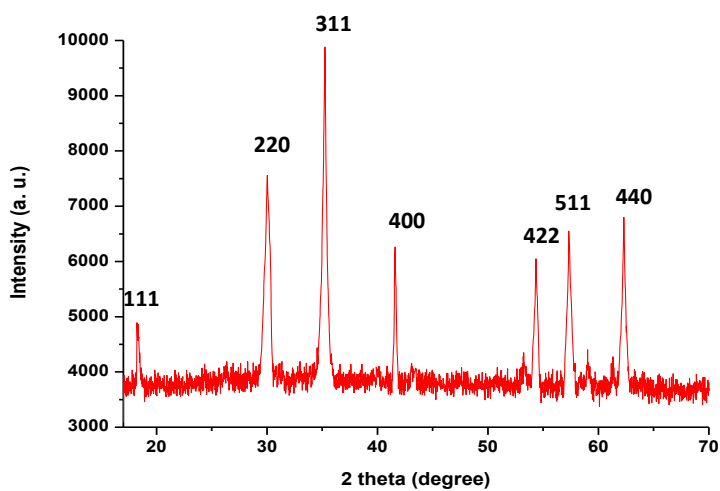


Fig. S13 Representative XRD diffraction patterns of Fe_3O_4 nanoparticles prepared by derivative 3.

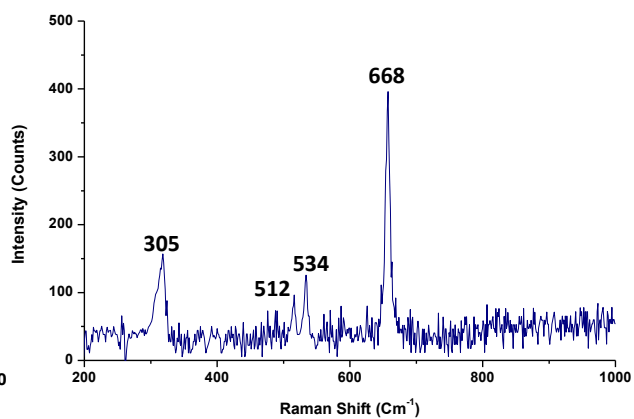


Fig. S14 Raman spectra of Fe_3O_4 nanoparticles prepared by derivative 3.

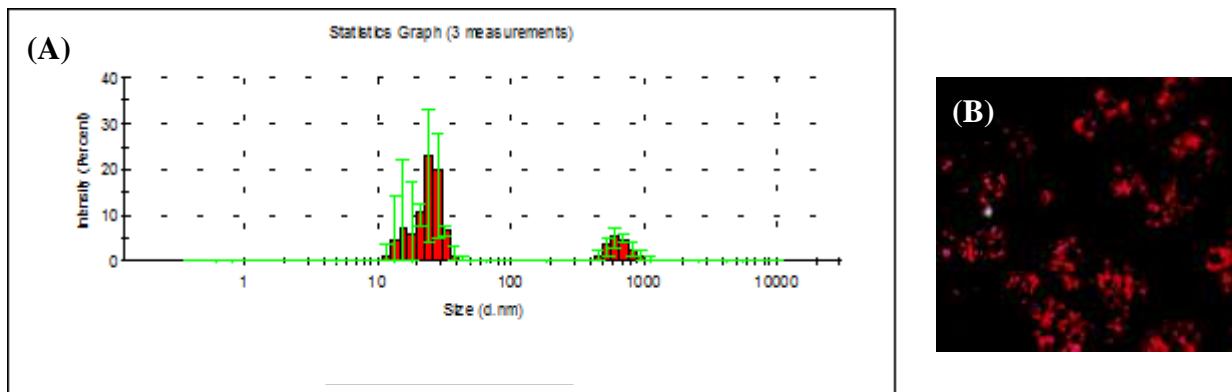


Fig. S15 (A) Dynamic light scattering (DLS) and (B) Polarized optical micrographs (POM) results of derivative **3** in H₂O/THF (3:7, v/v) mixture after the addition of Fe²⁺ ion.

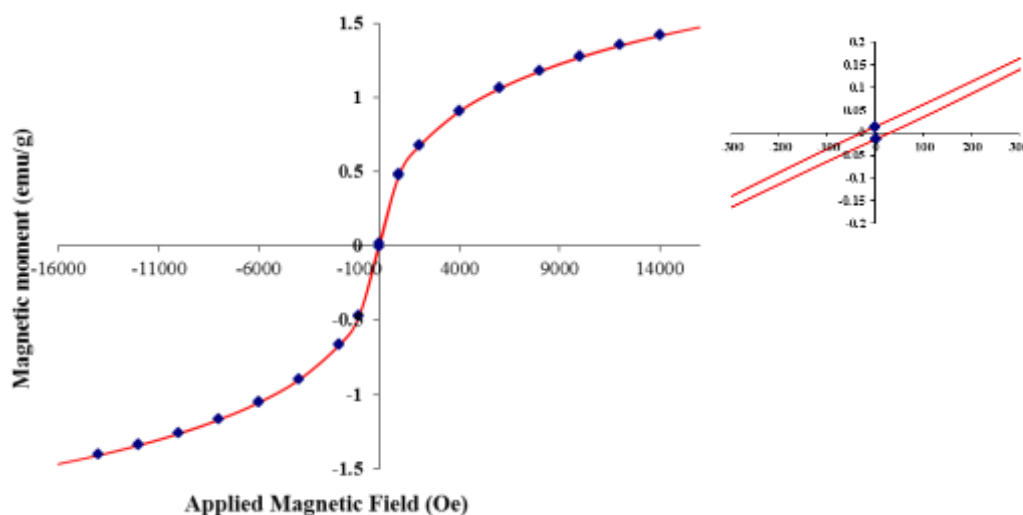


Fig. S16 Hysteresis loops of Fe₃O₄ nanoparticles at room temperature, 25°C.

	Upward Part	Downward part	Average	Parameter 'definition'
Hysteresis Loop				Hysteresis Parameters
Hc Oe	30.114	-28.042	29.078	Coercive Field: Field at which M/H changes sign
Mr emu	-731.199E-6	680.748E-6	705.973E-6	Remanent Magnetization: M at H=0
S	0.010	0.009	0.010	Squareness: Mr/Ms
S*	0.050	0.095	0.072	1-(Mr/Hc)(1/slope at Hc)
Ms emu	73.583E-3	-73.377E-3	73.480E-3	Saturation Magnetization: maximum M measured
M at H max emu	73.583E-3	-73.377E-3	73.480E-3	M at the maximum field

Saturation magnetization (M_S) = 3.67 emu g⁻¹, Remnant magnetization (M_r) = 0.035 emu g⁻¹ and coercivity force (Hc) = 29.08 Oe.

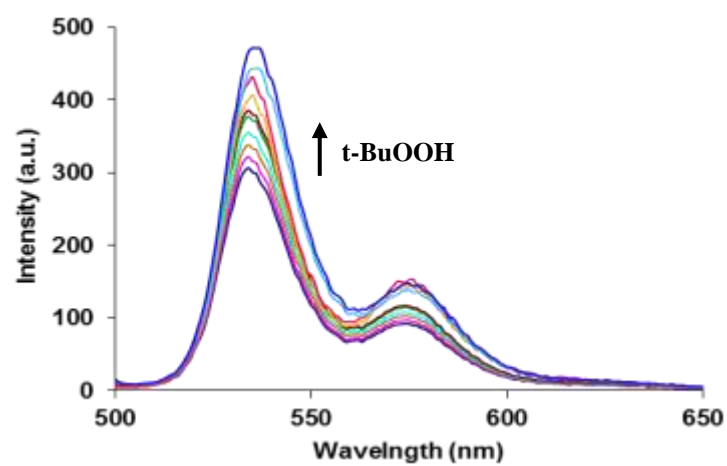


Fig. S17 Fluorescence emission spectra of derivative 3 ($5\mu\text{M}$) upon additions of 35 equiv. of 70 wt% tert-butyl hydroperoxide solution in $\text{H}_2\text{O}/\text{THF}$ (3/7) mixture.

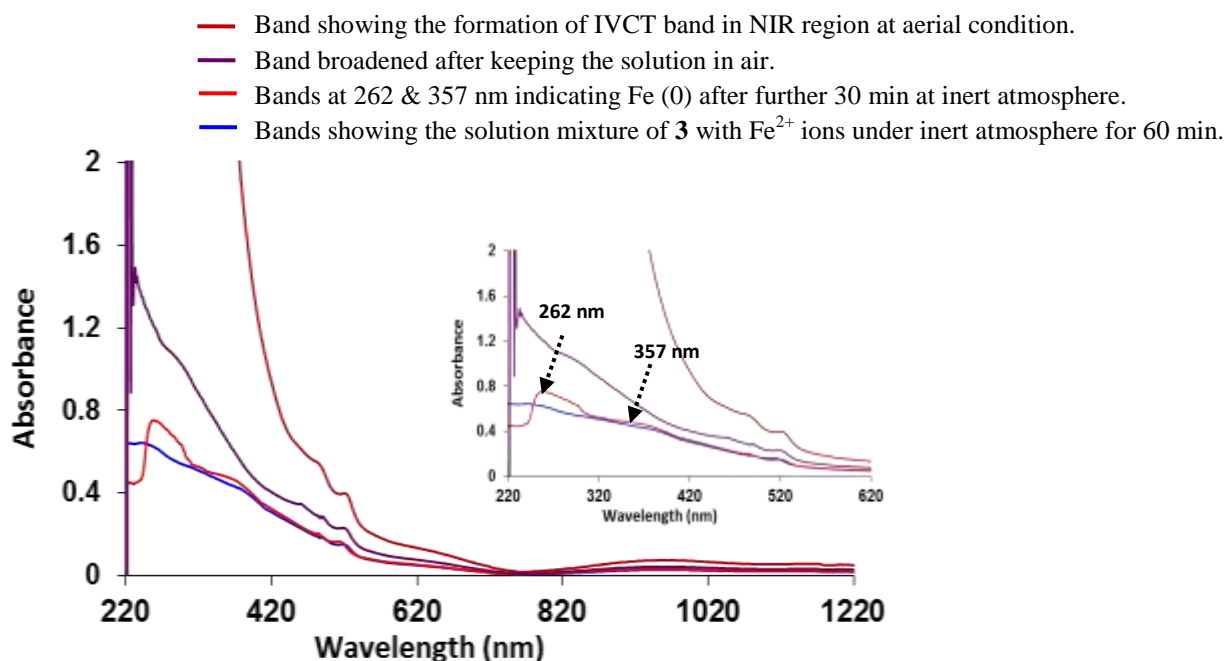


Fig. S18 UV-Vis-NIR Spectra showing the formation of Fe (0) Nps bands after keeping the solution of derivative **3** and Fe²⁺ ion (0-35 equiv.) in H₂O/THF (3:7, v/v) mixture under inert atmosphere for 90 min; Inset photographs showing *in situ* formation Fe (0) nanoparticle.

To prove the formation of Fe (0) in the reaction, we studied the reaction between aggregates of derivative **3** and FeCl₂ under inert atmosphere by UV-Vis-NIR spectroscopy. After 90 minutes of the reaction, the UV-Vis-NIR spectrum of the solution showed the presence of two bands at 262 and 357 nm corresponding to Fe (0) NPs. After keeping the sample under air, absorption band corresponding to Fe₃O₄ NPs appeared. This result clearly indicates the oxidation of Fe (0) NPs to Fe₃O₄ NPs.

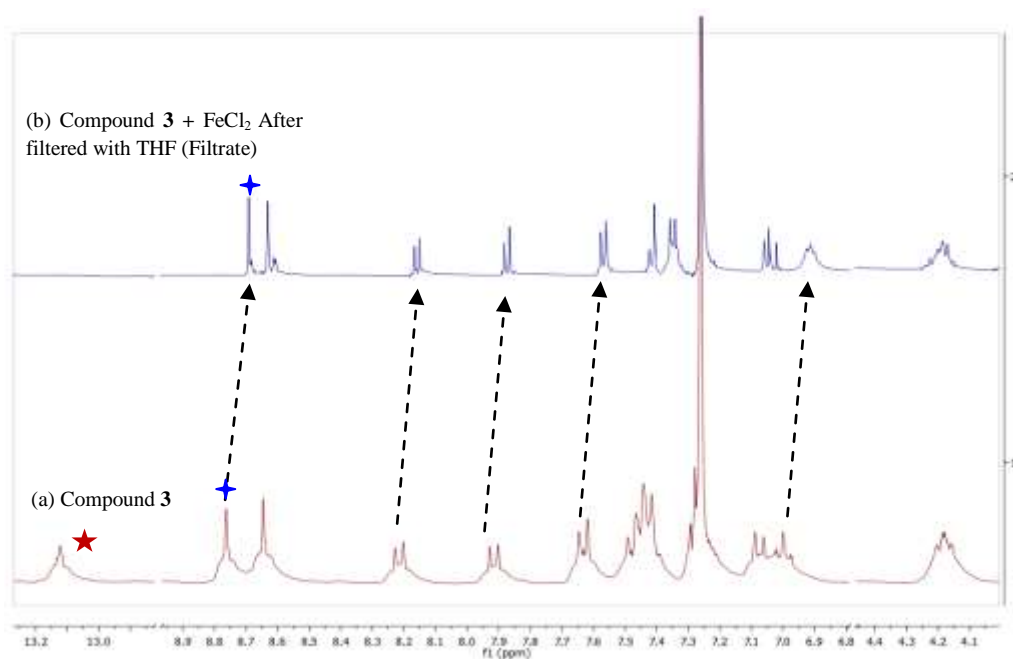


Fig. S19 Overlay ^1H NMR spectra of (a) compound **3** and (b) compound **3** + FeCl_2 after filtration with THF in CDCl_3 .

(a) Compound 3 (δ_3 , ppm)	(b) Compound 3 + Fe^{2+} , after filtration by THF (δ_F , ppm)	$\Delta\delta_1 = \delta_3 - \delta_F$
★ 13.13 (s, -OH)	Disappear	-
+ 8.77 (s, -N=CH)	8.68	0.09
8.65 (s, aromatic)	8.58	0.07
8.22 (d, aromatic)	8.16	0.06
7.92 (d, aromatic)	7.87	0.05
7.63 (d, aromatic)	7.58	0.05
7.50-7.42 (m, aromatic)	7.48-7.35	0.04
7.08 (d, aromatic)	7.02	0.06
7.02 (d, aromatic)	6.94	0.08

Table S6: Change in chemical shift (δ) value of ^1H NMR spectra of derivative **3** in CDCl_3 and Fe_3O_4 nanoparticles of derivative **3** after filtration with THF.

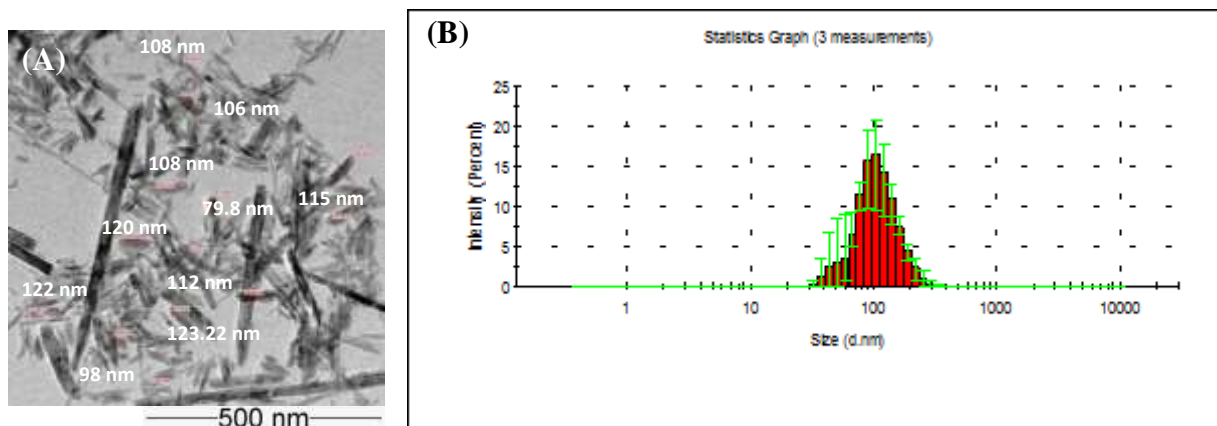


Fig. S20 (A) TEM (Scale bar 500 nm) and (B) DLS analysis of compound **3** (5 μM) showing the size of Fe_3O_4 nanorods at temperature 60°C in the range of 80-120 nm

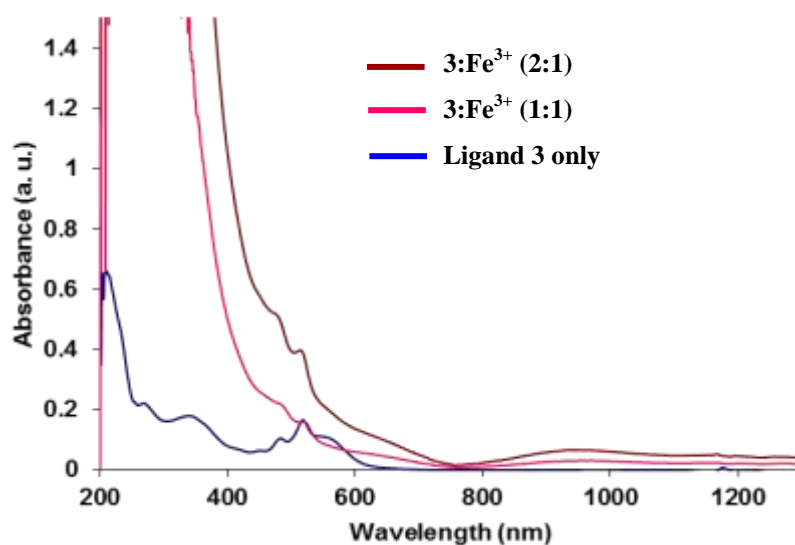


Fig. S21 UV-vis-NIR spectra of compound **3** (5 μM) on addition of Fe^{2+} ions (0-35 equiv.) in 2:1 ratio showing the formation of IVCT band (180 minutes) in $\text{H}_2\text{O}/\text{THF}$ (3:7, v/v) mixture

Upon heating the mixture of derivative **3** and Fe^{2+} ions in $\text{H}_2\text{O}/\text{THF}$ (3:7, v/v) at 60°C , the nanorods of size in the range of 80-120 nm were obtained (Fig. S19). The UV-vis-NIR studies show that when aggregates of derivative **3** and Fe^{2+} ions are mixed in 2:1 ratio, rate of formation of nanorods is increased (180 minutes) (Fig. S20).

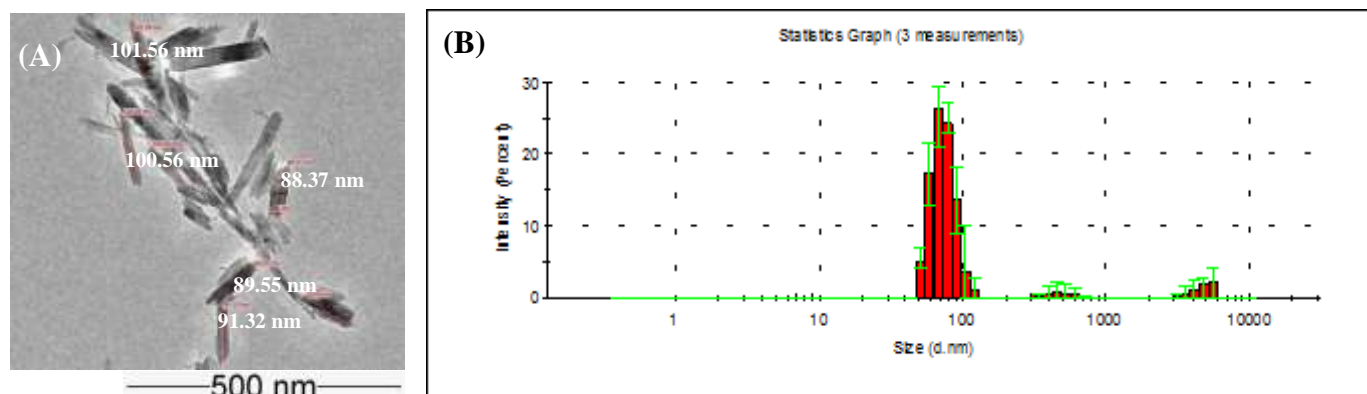


Fig. S22 (A) TEM images Scale bar 500 nm (B) DLS of Fe_3O_4 nanoparticles (average size ~80-100 nm) prepared by using 2:1 mixture of derivative **3** and Fe^{2+} ions

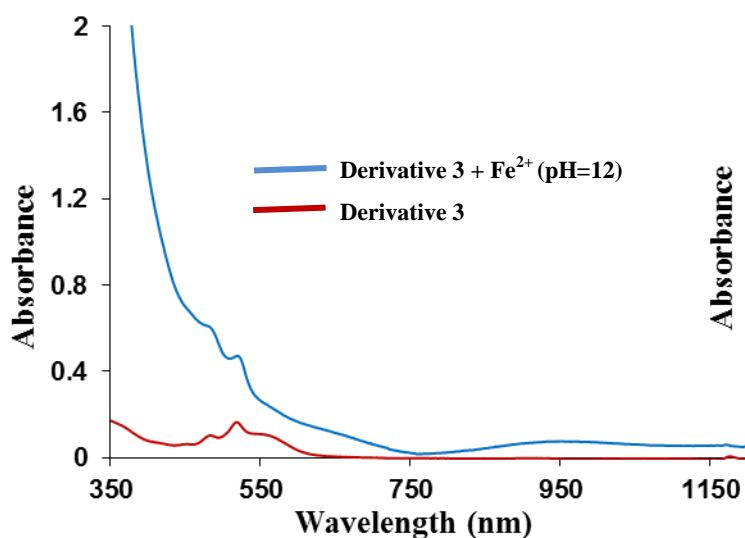


Fig. S23A UV-vis-NIR spectra of compound **3** ($5 \mu\text{M}$) showing the formation of IVCT band (45 minutes) at pH=12 solution after addition of Fe^{2+} ions (0-35 equiv.) in $\text{H}_2\text{O}/\text{THF}$ (3:7, v/v) mixture

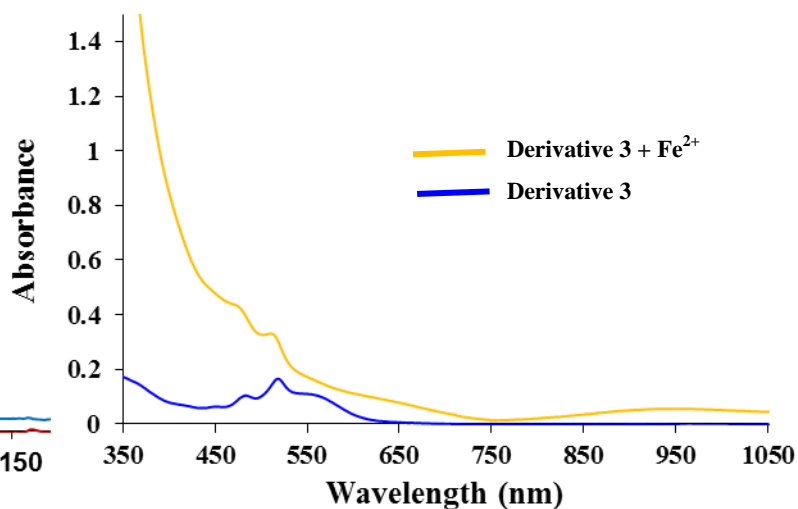


Fig. S23B UV-vis-NIR spectra of compound **3** ($5 \mu\text{M}$) showing the formation of IVCT band (210 minutes) in on addition of Fe^{2+} ions (0-35 equiv.) in MeOH/THF (3:7, v/v) mixture

TEM and DLS analysis of this sample of aggregates of derivative **3** and Fe^{2+} ions mixed in 2:1 ratio show the presence of nanorods of size in the range of 80-100 nm (Fig. S21). Further, in the presence of sodium hydroxide (pH=12) and methanol, the UV-vis-NIR studies show the rate of formation of nanorods after 45 and 210 minutes (Fig. S22 A-B, ESI†).

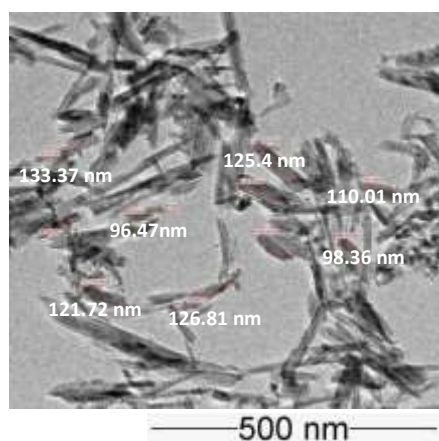


Fig. S24 (A) TEM (Scale bar 500 nm) of compound **3** (5 μ M) showing the size of Fe_3O_4 nanorods at pH=12 in the range of 80-130 nm.

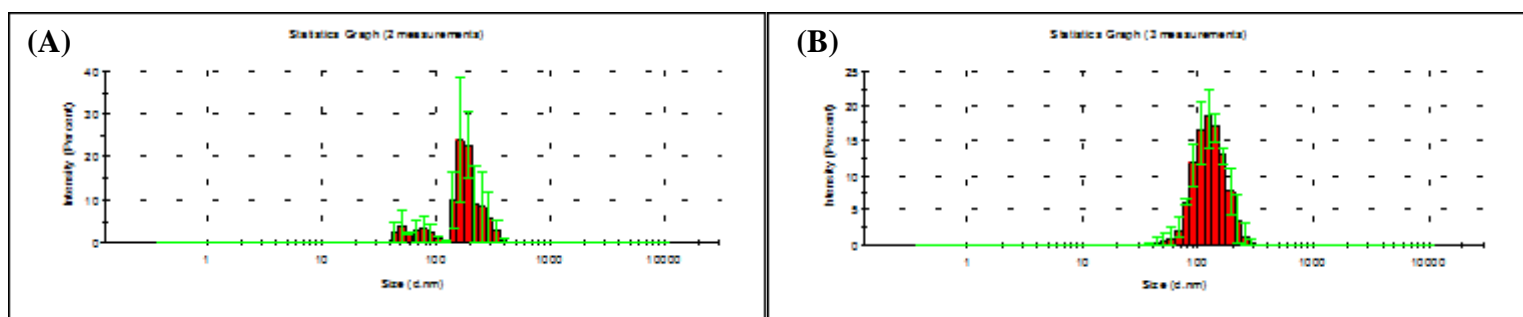


Fig. S25 DLS analysis of compound **3** (5 μ M) showing the size of Fe_3O_4 nanorods at (A) pH=12 having size -80-130 nm; (B) in Methanol/THF (3:7, V/V) having size -80-140 nm.

TEM image of derivative **3** and Fe^{2+} ions in the presence of sodium hydroxide (pH=12) show the presence of nanorods having size in the range of 80-130 nm (Fig. S23). DLS studies in the presence of sodium hydroxide (pH=12) and methanol, show the presence of nanorods of average size in the range of 80-130 nm (Fig. S24A-B, ESI†).

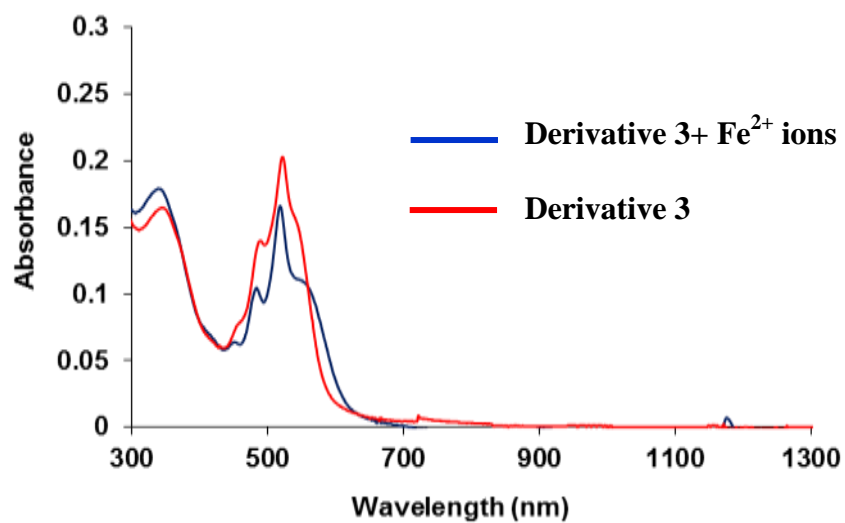


Fig. S26 UV-vis-NIR spectra of compound **3** (5 μ M) on addition of Fe^{2+} ions (0-35 equiv.) in THF (3:7, v/v) mixture

Entry	Solvents	Temperature	Yield (%) ^a
1	Solvent Free/Neat	r.t.	89
2	Toluene	120	80
3	THF	60	68
4	Acetonitrile	80	59
5	Ethanol	80	20

Table S7: Solvent effect on A^3 -coupling reaction in model reaction of benzaldehyde (1.0 equiv), piperidine (1.2 equiv) and phenylacetylene (1.2 equiv) in the presence Fe_3O_4 nanoparticles (0.5 mol%), solvent (5.0 mL) at the different temperature.

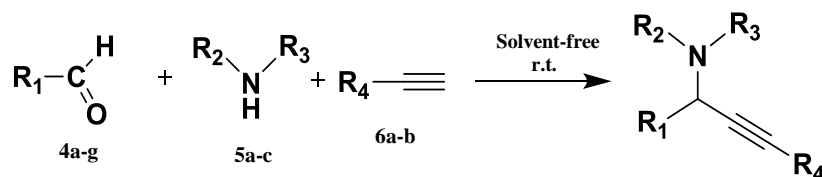
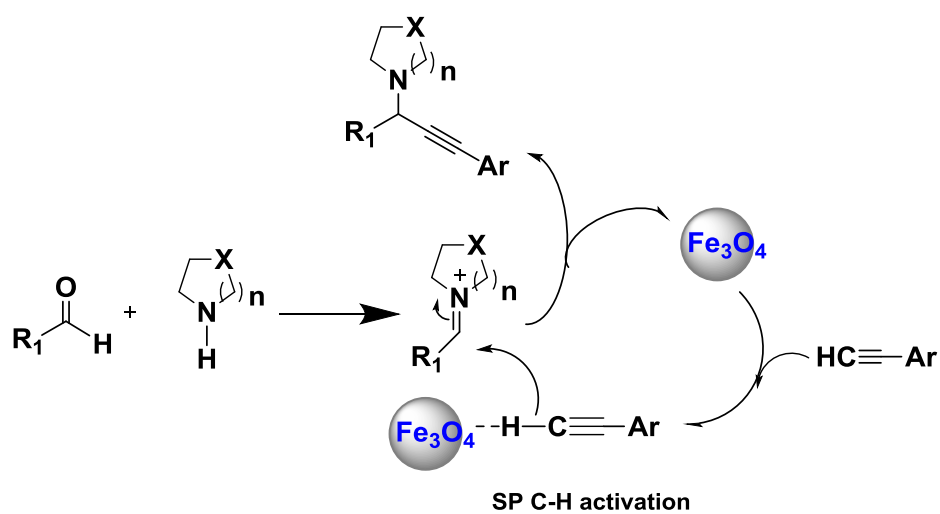


Table S8. *In situ* generated Fe₃O₄ nanoparticles catalysed A^{3a-j}-coupling reaction of various aldehyde, amines and alkynes to give corresponding products

Entry	Aldehyde	Amine	Alkyne	Product	Time (h)	(%) Yield
1 ^{a,b,c}					24h ^a 16h ^b 3.5h ^c	40 ^a 82 ^b 89 ^c
2					3h	92
3					5h	86
4 ^d					5h	62
5					4.5	81
6					4	84
7	HCHO				4.5	81
8					3.0	93
9					4.5	83
10					5h	72

Reaction condition: entry 1^a Bare Fe₃O₄ nanoparticles, entry 1^b solution of aggregates of **3**, Fe²⁺ in 2:1 ratio, entry 1^c solution of aggregates of **3** and Fe²⁺ in 1:1 ratio; Neat (0.5 mol%) at r.t. for all reactions except for entry 4^d 50°C in toluene (5 ml), catalyst (1 mol%)



Scheme S1 Tentative mechanism of Fe_3O_4 nanoparticles catalyzed A^3 -coupling.

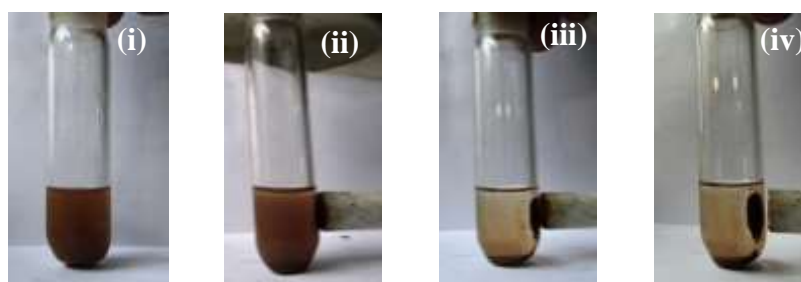


Fig. S27 Fe_3O_4 nanoparticles (i) dispersed in the reaction mixture; (ii) a magnetic stirring bar put towards the reaction mixture (entry 1c, table S8); (iii-iv) after 30 sec an external magnet attracted Fe_3O_4 nanoparticles.

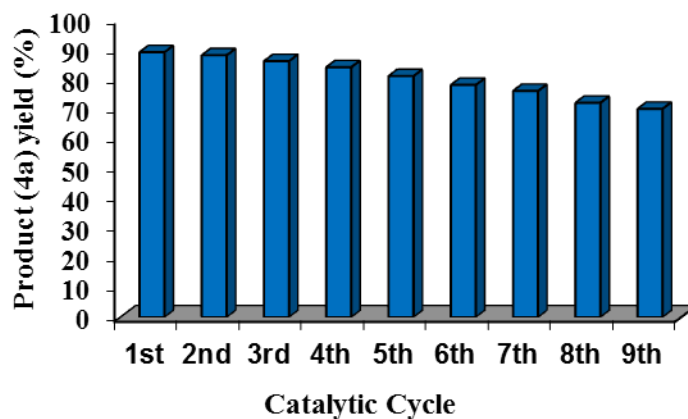


Fig. S28 Recyclability of the Fe₃O₄ nanoparticles catalyst in A³-coupling reaction of benzaldehyde (4a), piperidine (5a) and phenylacetylene (6a) (entry 1c, table S8)

Entry	Fe ₃ O ₄ NPs (ppm)	Time (hours)	Yield (%)	TON	TOF (h ⁻¹)
1	5000 (0.5 mol%)	3.5	89	17.8	5.08
2	1000 (0.1 mol%)	5.5	86	86	15.63
3	100 (0.01 mol%)	8	82	820	102.5
4	10 (0.001 mol%)	11	80	8000	727.27
5	0 mol%	24	0	0	0

Table S9: Fe₃O₄ nanoparticles catalysed A³ coupling reaction of benzaldehyde (4a), piperidine (5a) and phenylacetylene (6a) using various amounts of Fe₃O₄ nanoparticles.

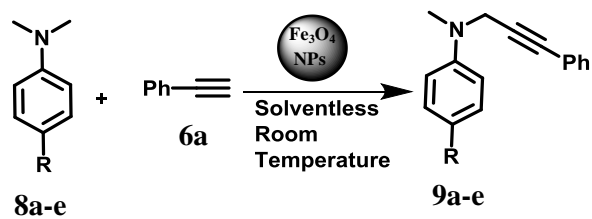


Table S10: *In situ* generated Fe₃O₄ nanoparticles catalysed (1 mol%) propargylamine synthesis various substrates of N,N-alkyl anilines with phenylacetylene under aldehyde free conditions.

Entry	Aniline	Product	Time (min)	(%) Yields
1			3.5h	79
2			3h	86
3			4h	83
4			4.2h	78
5			4.5	76

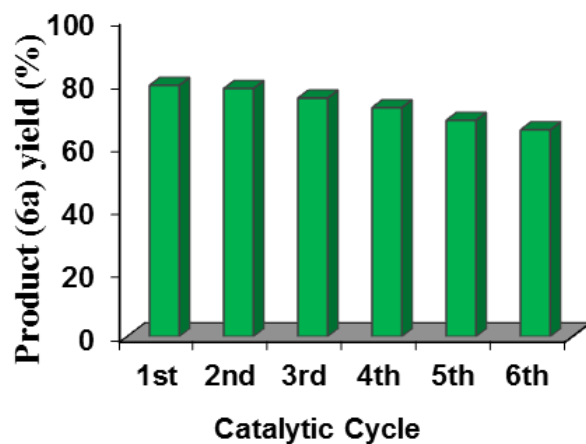
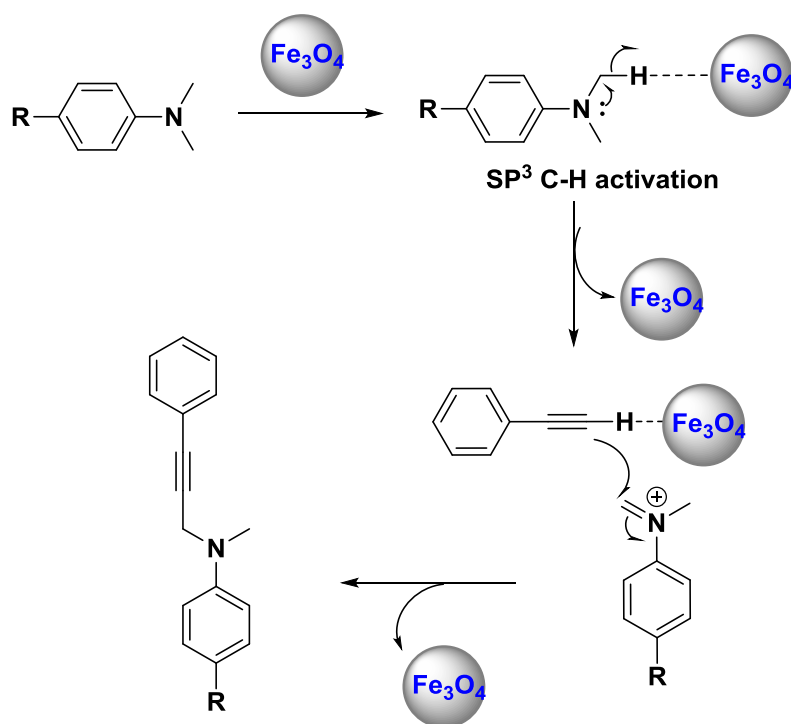


Fig. S29 Recyclability of Fe_3O_4 nanoparticles catalyst in aldehyde free synthesis of propargylamines (9a) through *N,N*-dimethyl aniline (8a) and phenylacetylene piperidine (6a).



Scheme S2 A plausible mechanism for aldehyde free propargylamine synthesis

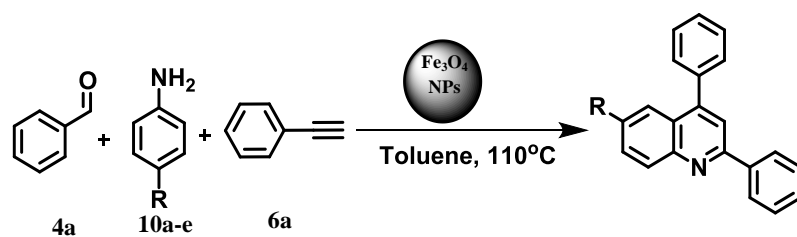


Table S11: *In situ* generated Fe_3O_4 nanoparticles catalysed quinoline synthesis utilizing various substrates of anilines with benzaldehyde and phenyl acetylene.

En try	Amine	Product	Time	% Yield
1	10a	11a	5h	84
2	10b	11b	3.5h	92
3	10c	11c	5h	83
4	10d	11d	4.5	90
5	10e	11e	6.5h	79

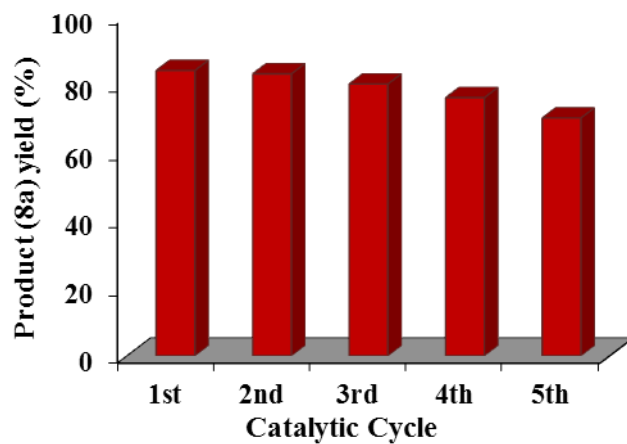
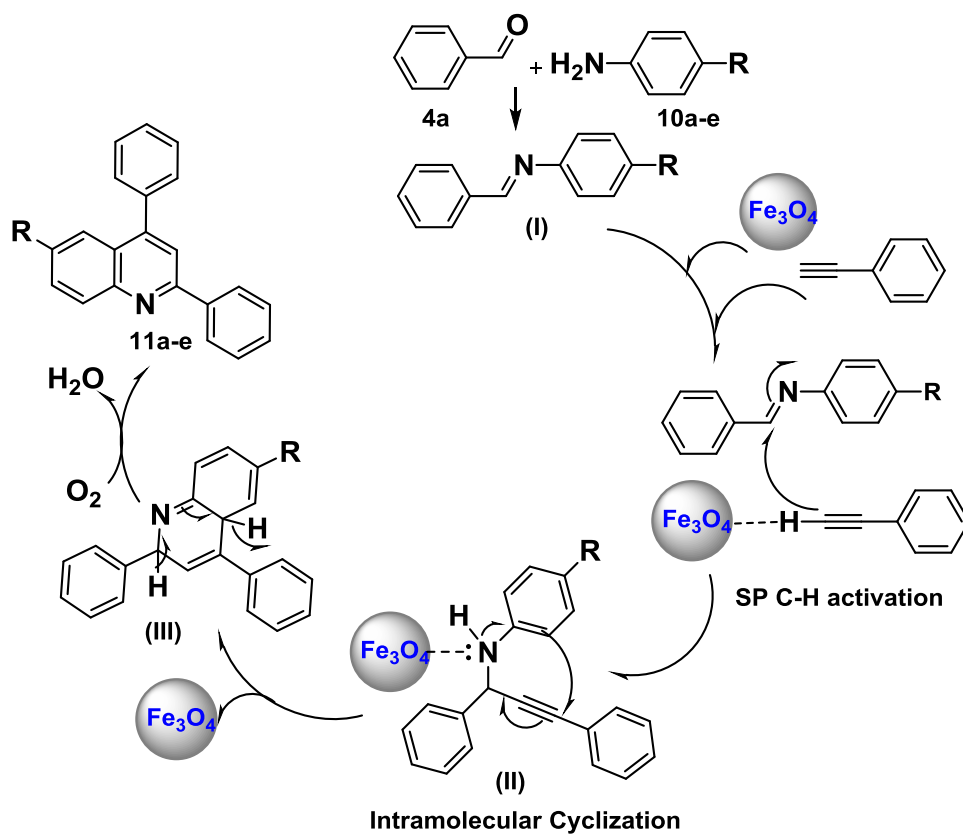


Fig. S30 Recyclability of Fe_3O_4 nanoparticles catalyst in synthesis of quinoline (**11a**) through benzaldehyde (**4a**), aniline (**10a**) and phenylacetylene (**6a**)



Scheme S3 A plausible mechanism for quinoline synthesis by Fe_3O_4 nanoparticles.

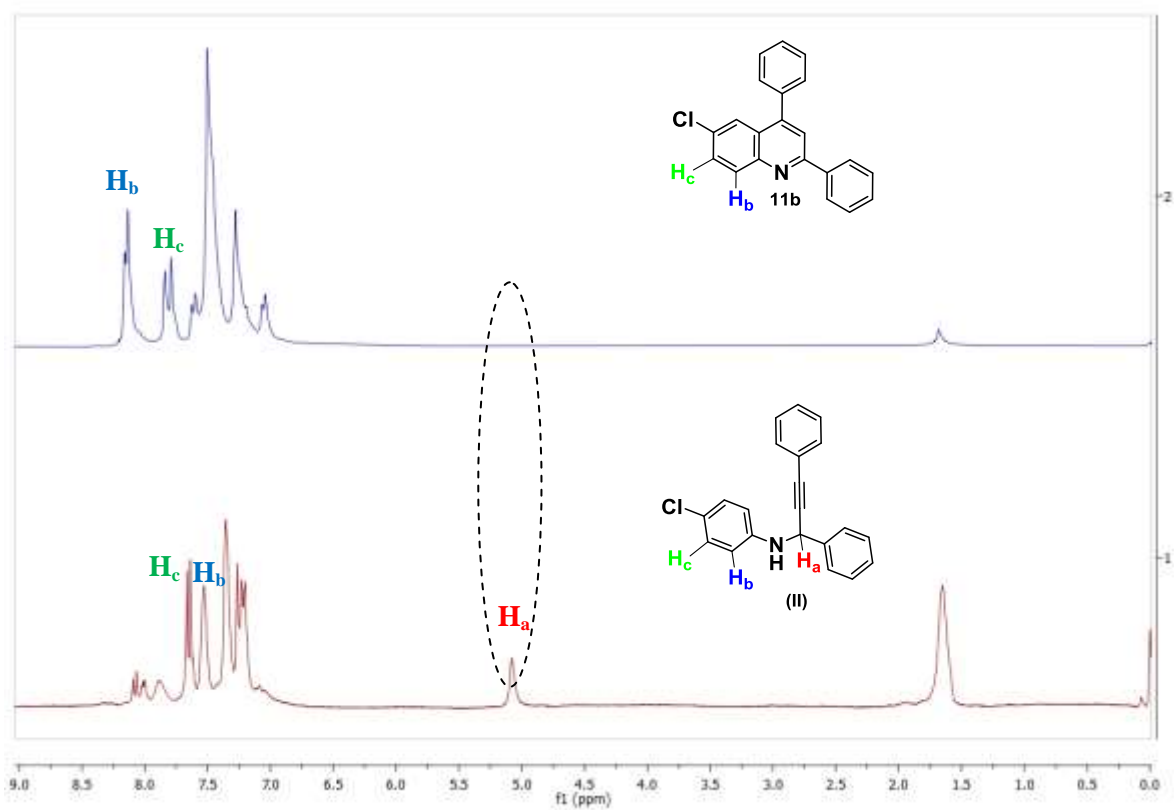


Fig. S31 ¹H NMR of (a) propargylamine intermediate generated in preparation of (b) quinoline derivative (**11b**).

^1H NMR spectrum of derivative **3** in CDCl_3

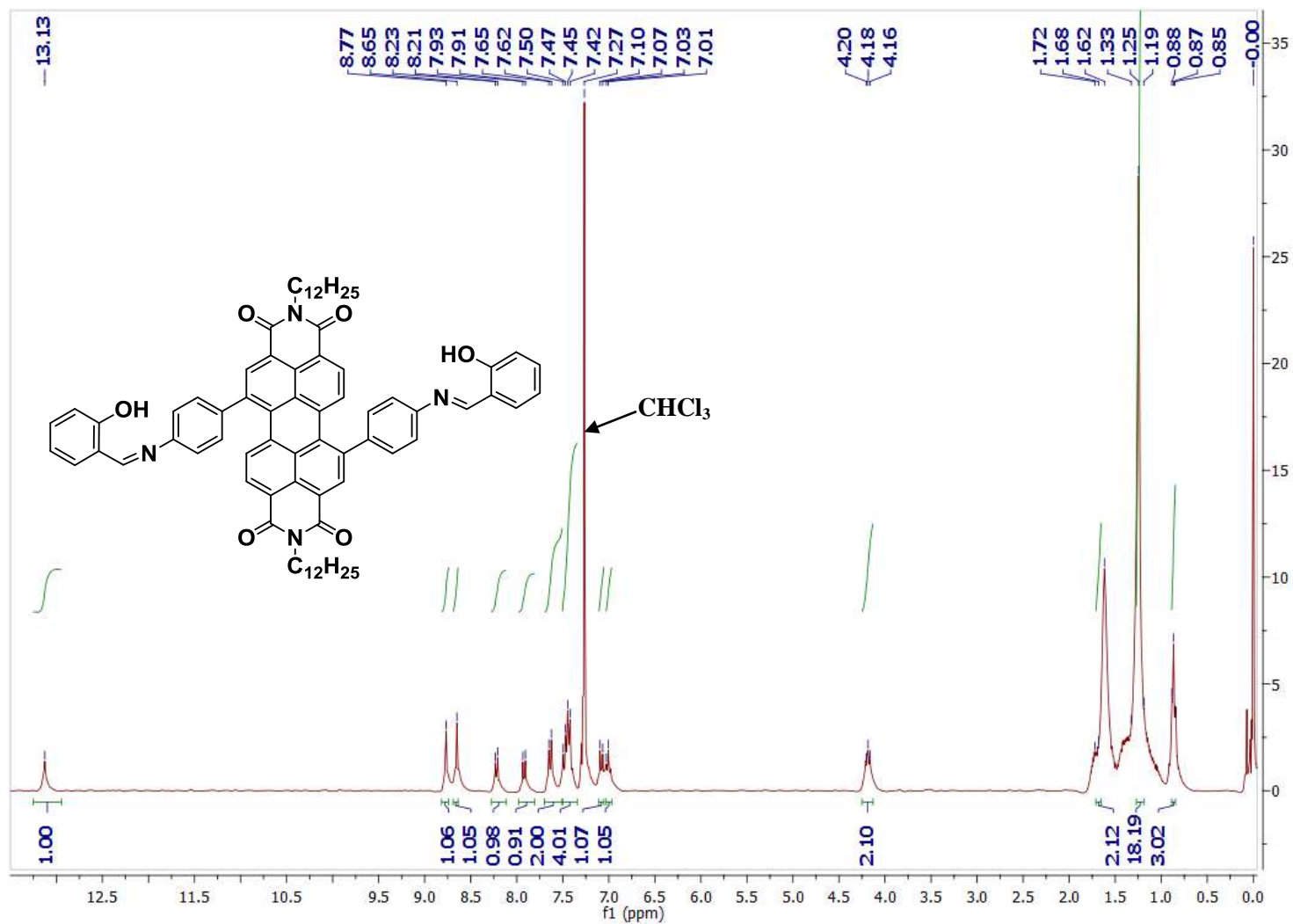


Fig. S32 ^1H NMR spectrum of derivative **3** in CDCl_3 .

^{13}C NMR spectrum of derivative **3** in CDCl_3

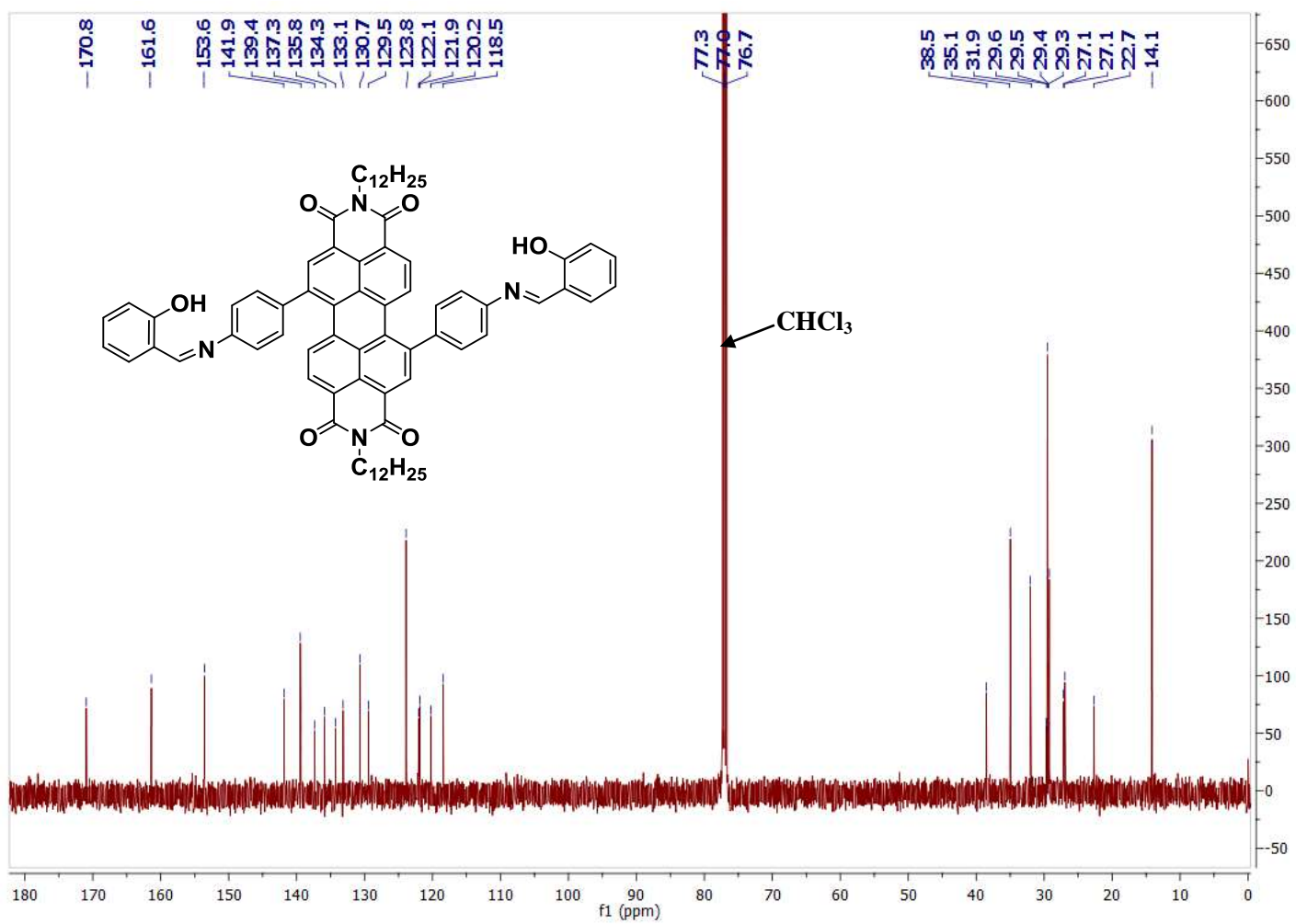


Fig. S33 ^{13}C NMR spectrum of derivative **3** in CDCl_3 .

ESI-MS Spectrum of compound 3:

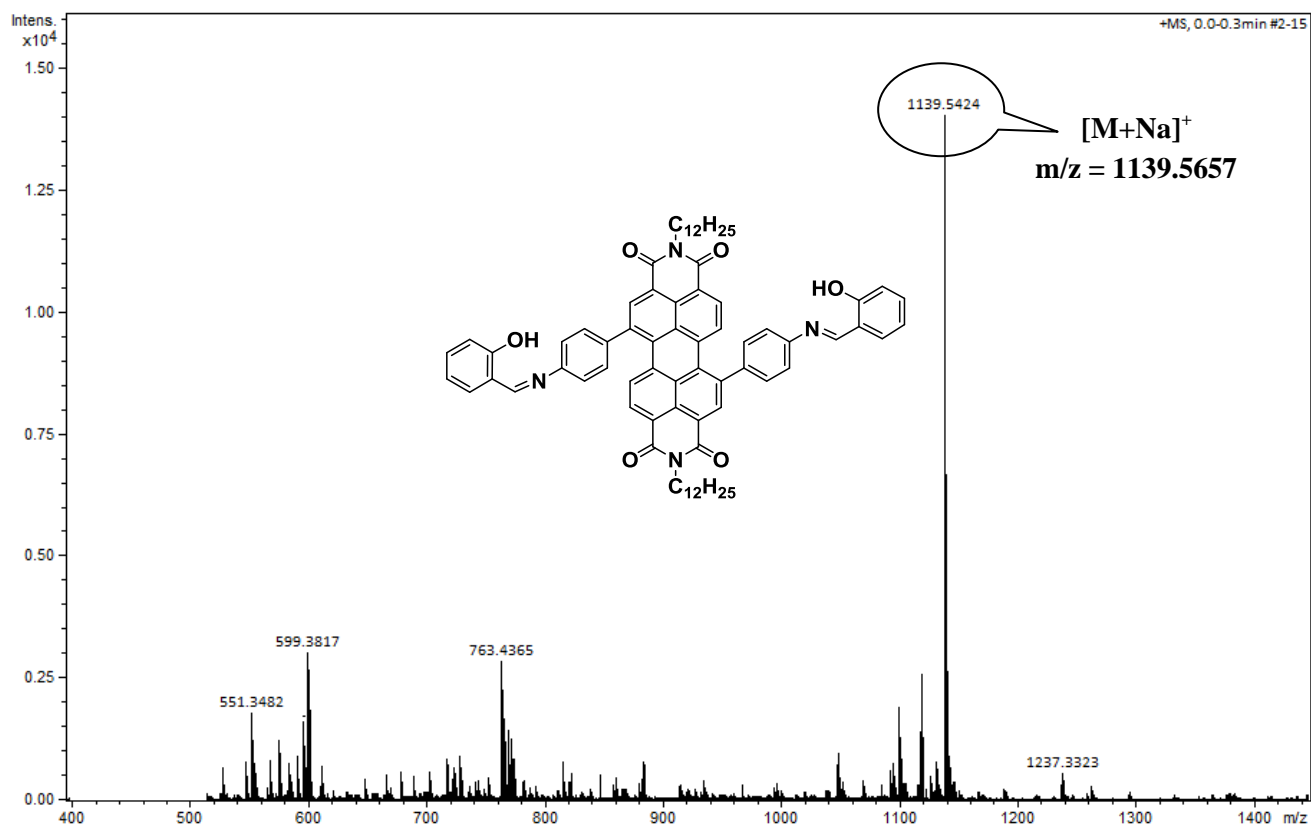


Fig. S34 ESI-MS Mass spectrum of derivative 3.

Fig. S35 ^1H NMR spectrum of derivative **7a** in CDCl_3

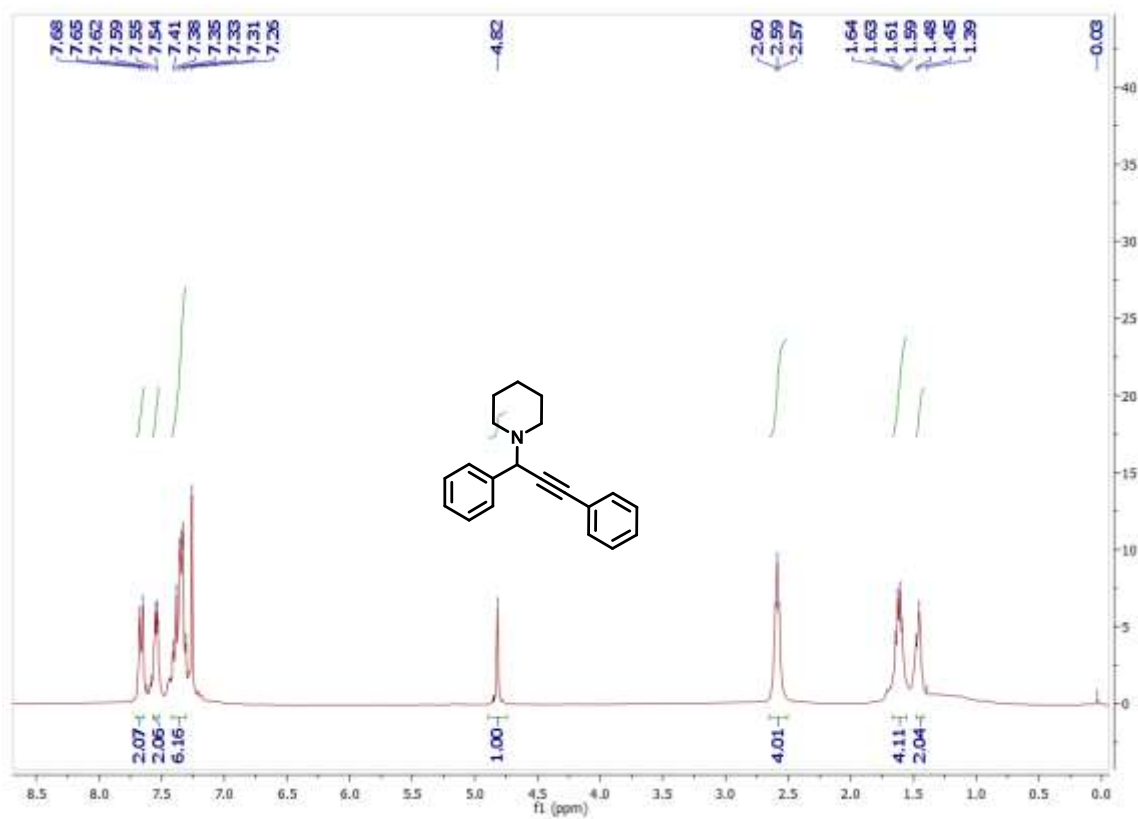


Fig. S36 ^1H NMR spectrum of derivative **7b** in CDCl_3

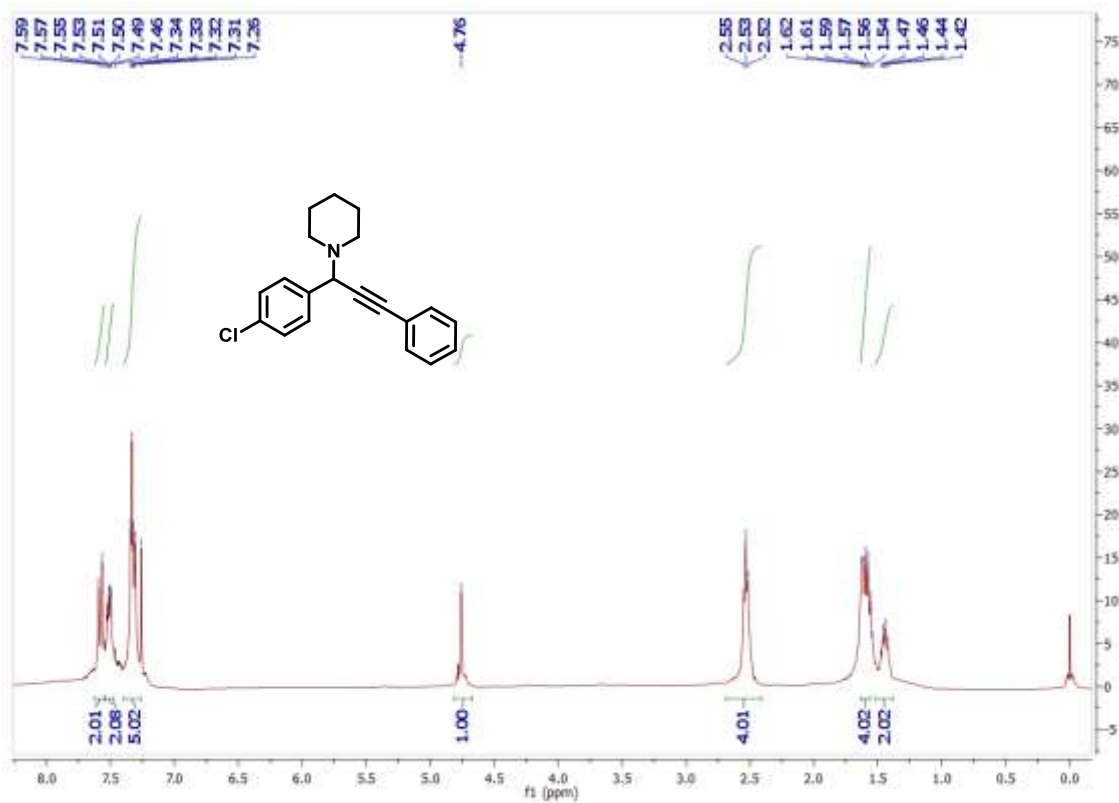


Fig. S37 ^1H NMR spectrum of derivative **7c** in CDCl_3

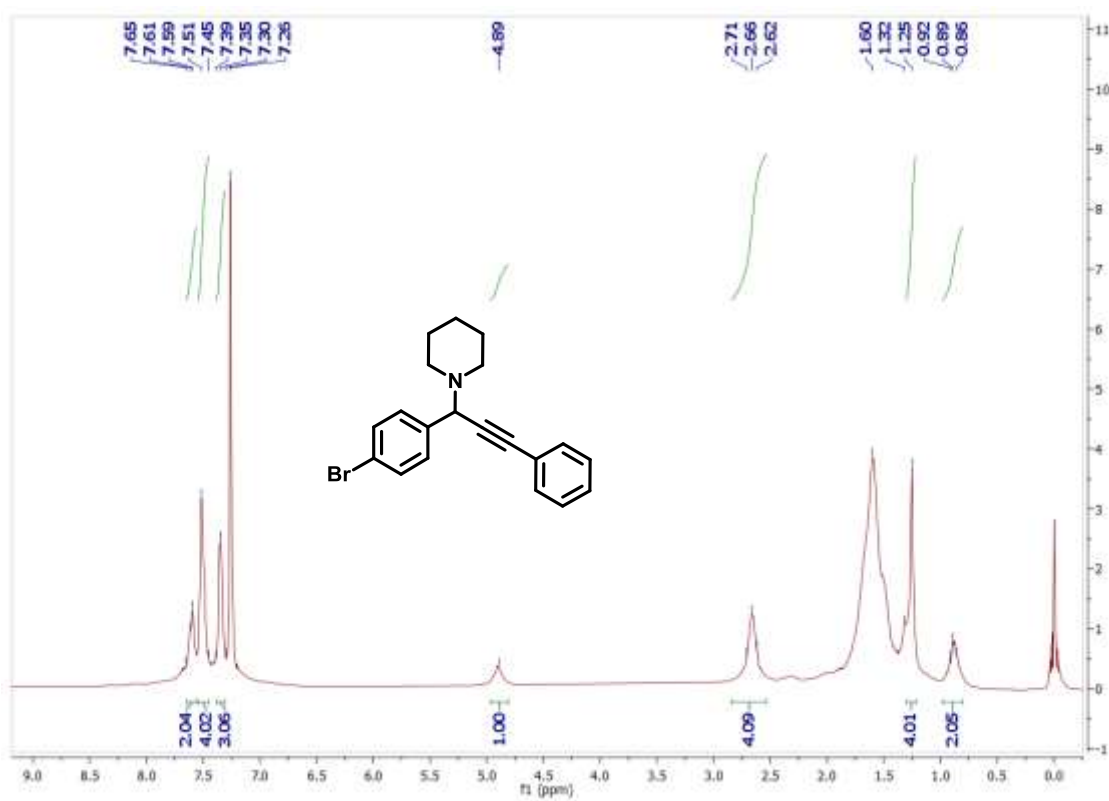


Fig. S38 ^1H NMR spectrum of derivative **7d** in CDCl_3

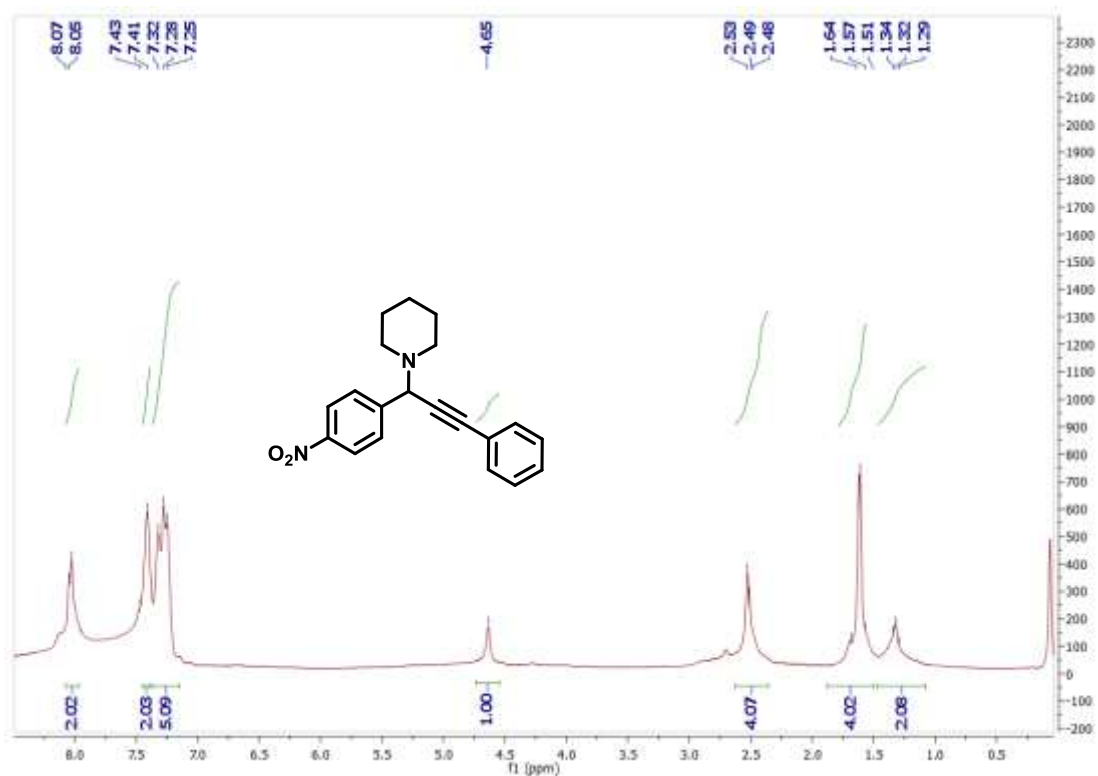


Fig. S39 ^1H NMR spectrum of derivative **7e** in CDCl_3

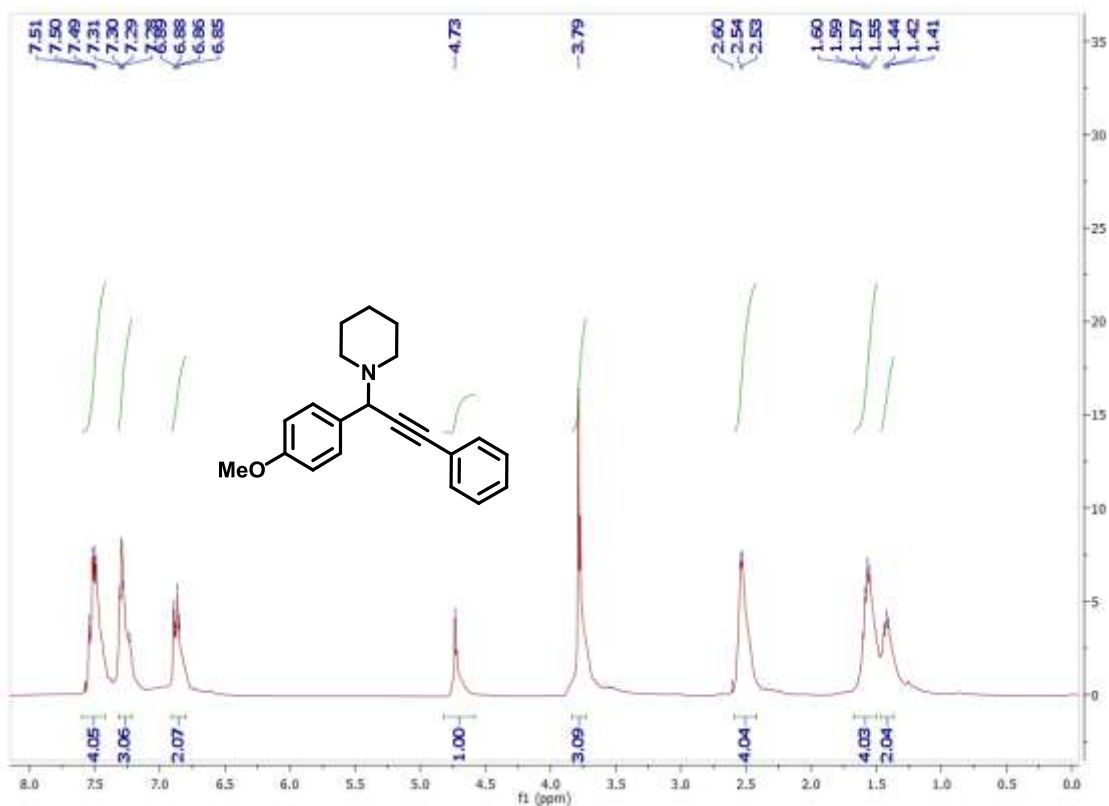


Fig. S40 ^1H NMR spectrum of derivative **7f** in CDCl_3

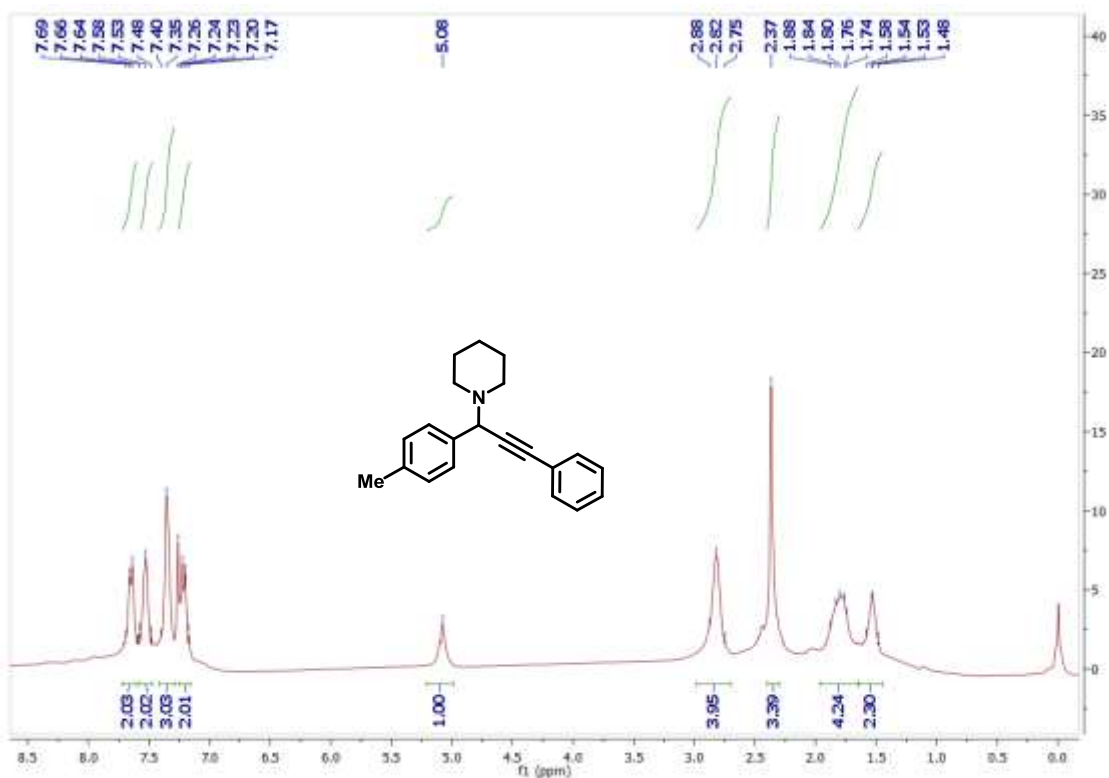


Fig. S41 ^1H NMR spectrum of derivative **7g** in CDCl_3

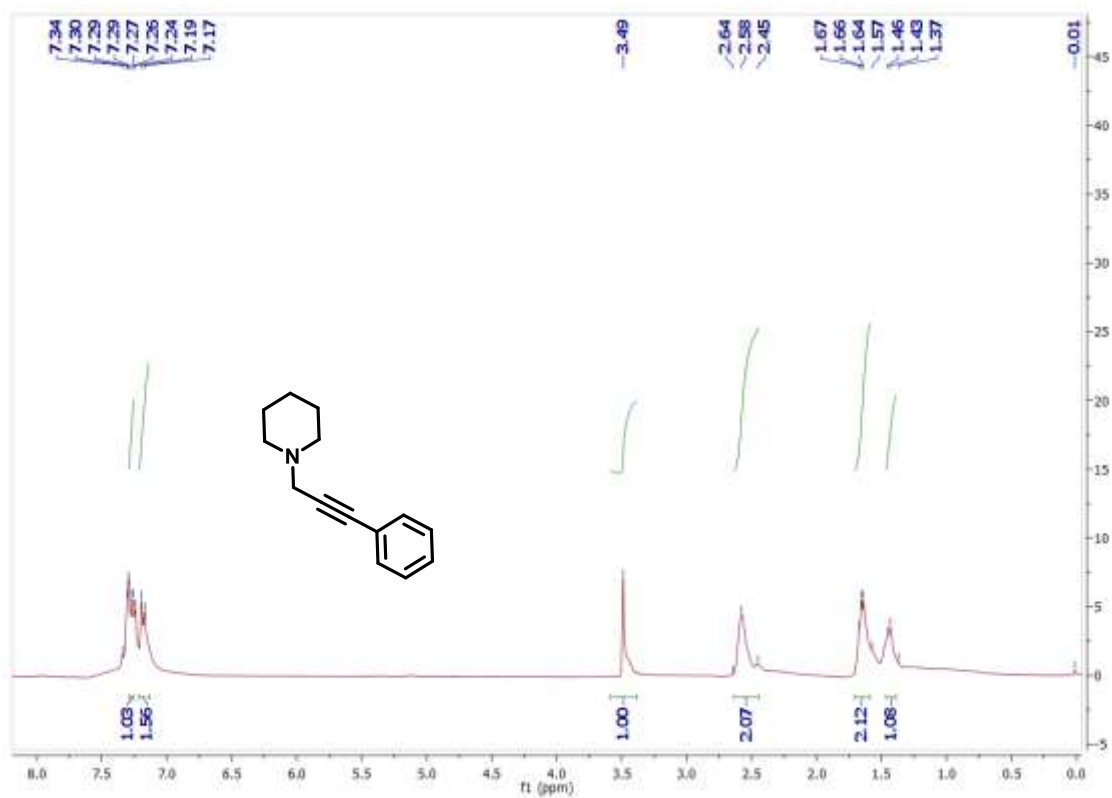


Fig. S42 ^1H NMR spectrum of derivative **7h** in CDCl_3

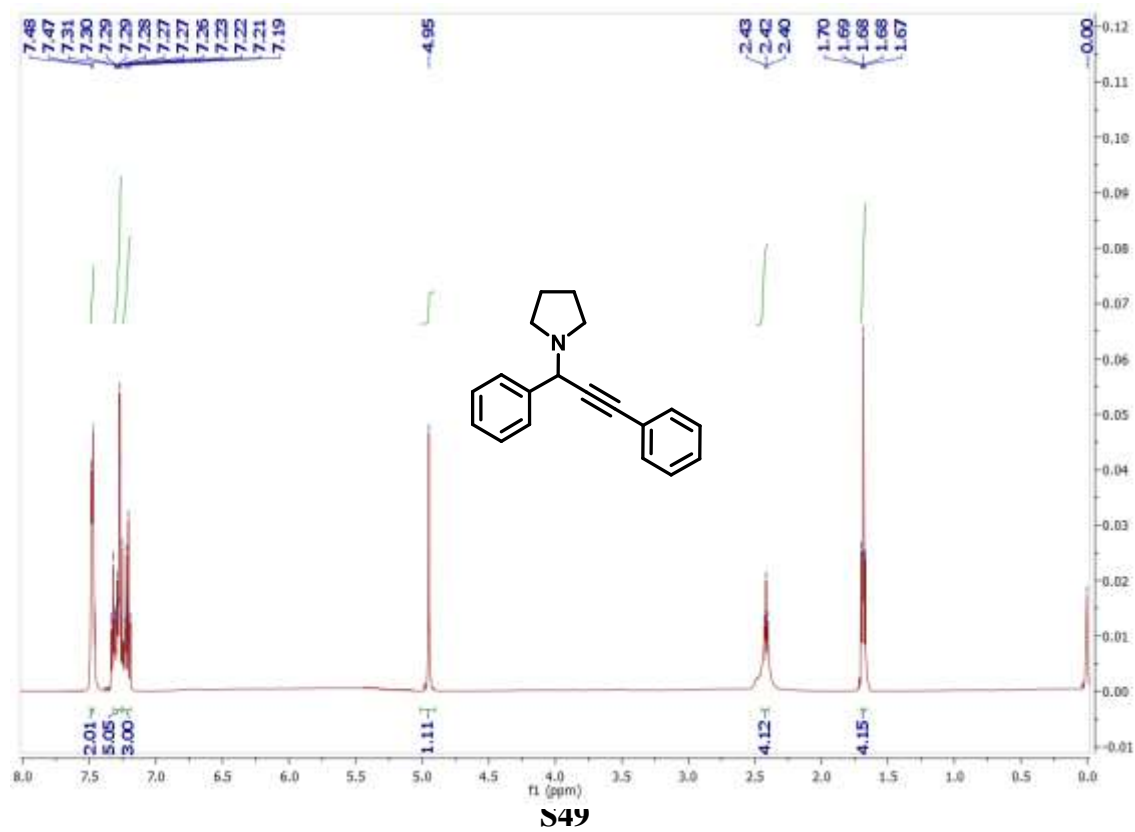


Fig. S43 ^1H NMR spectrum of derivative **7i** in CDCl_3

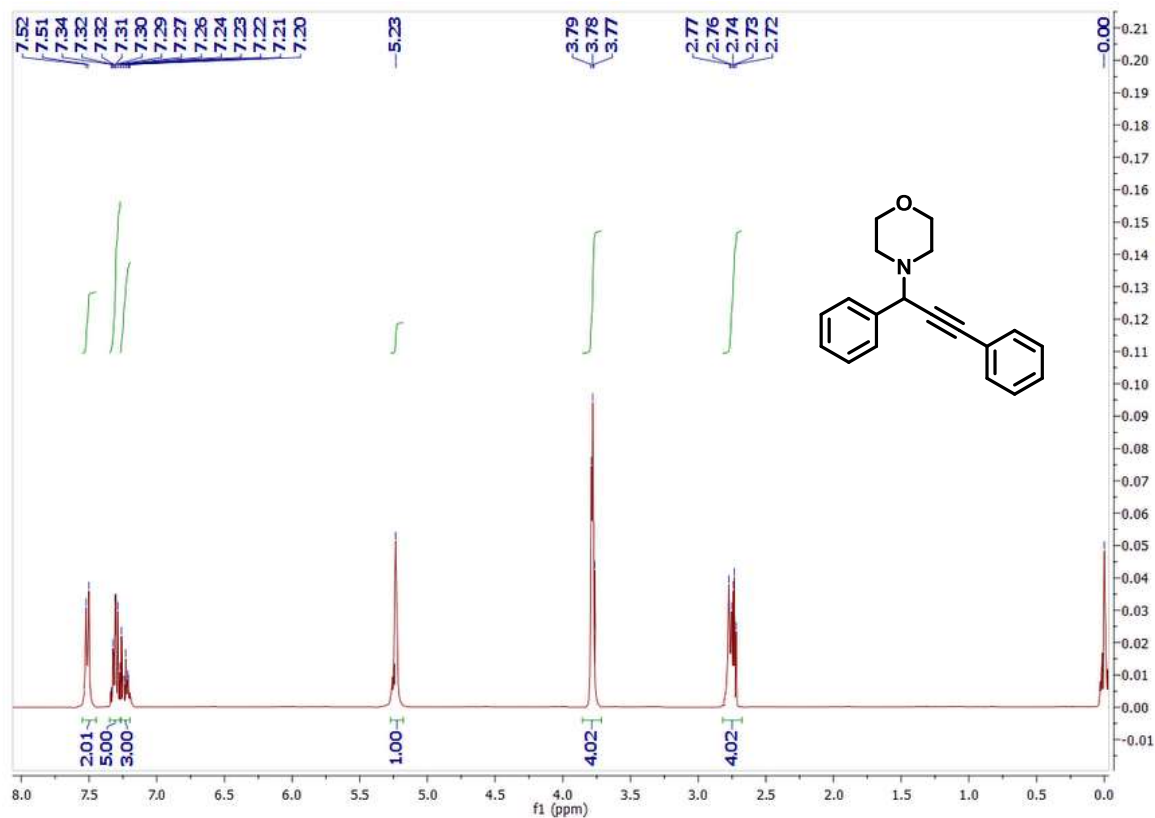


Fig. S44 ^1H NMR spectrum of derivative **7j** in CDCl_3

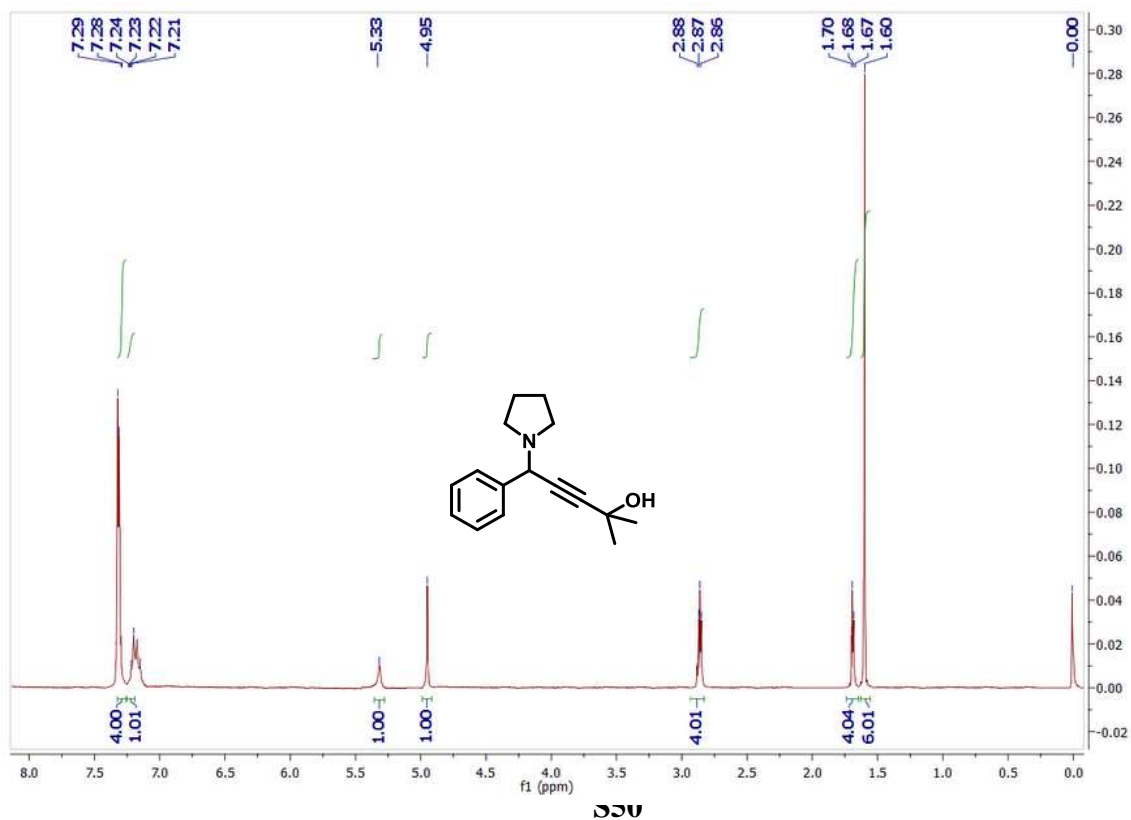


Fig. S45 ^1H NMR spectrum of derivative **4h** in CDCl_3

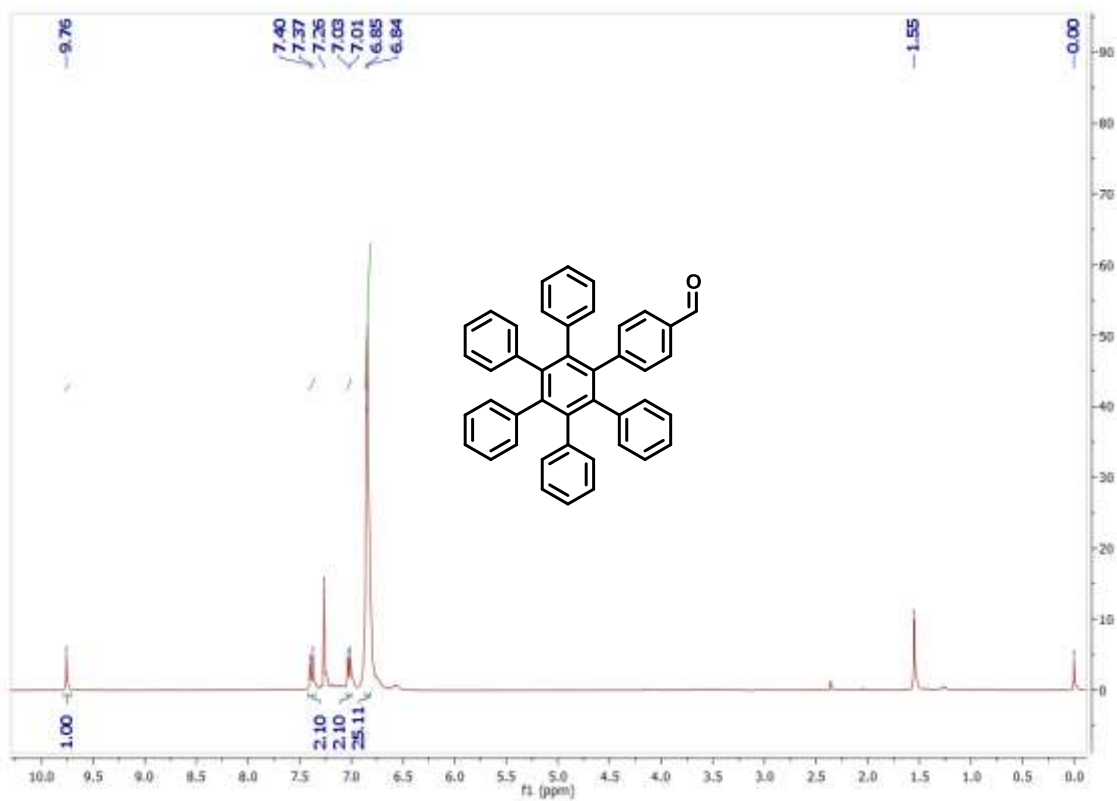


Fig. S46 ^1H NMR spectrum of derivative **7k** in CDCl_3

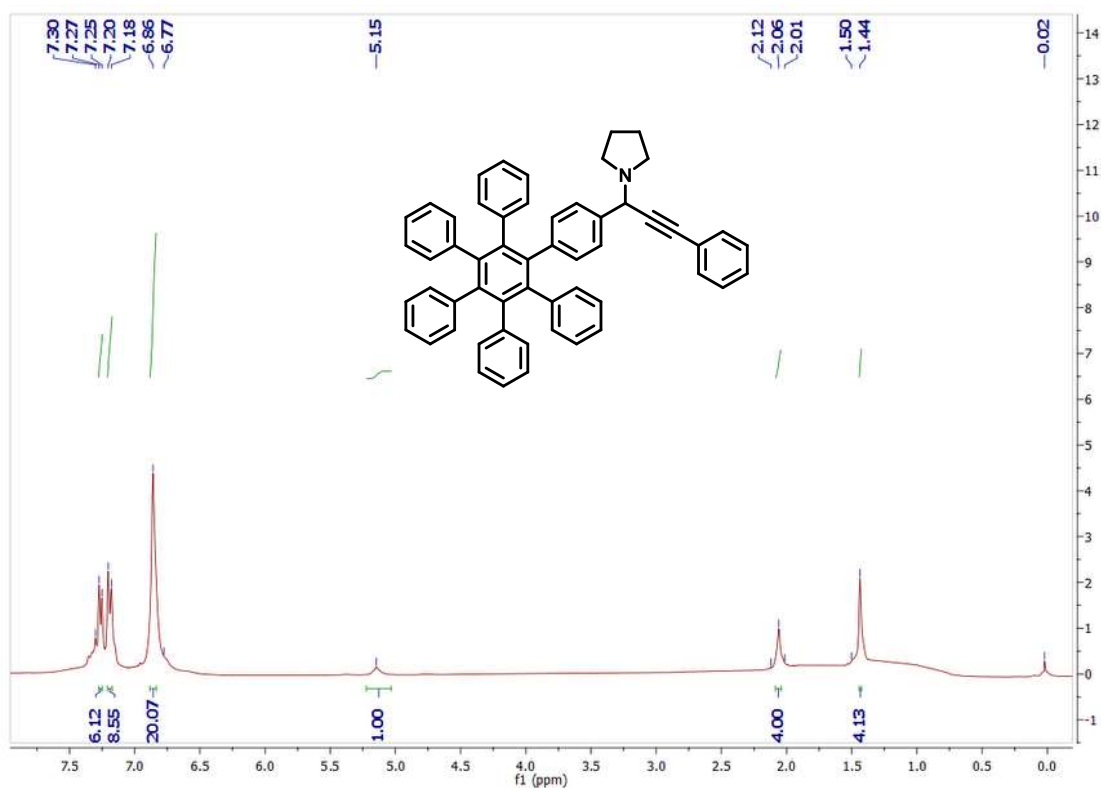


Fig. S47 ¹H NMR spectrum of derivative **9a** in CDCl₃

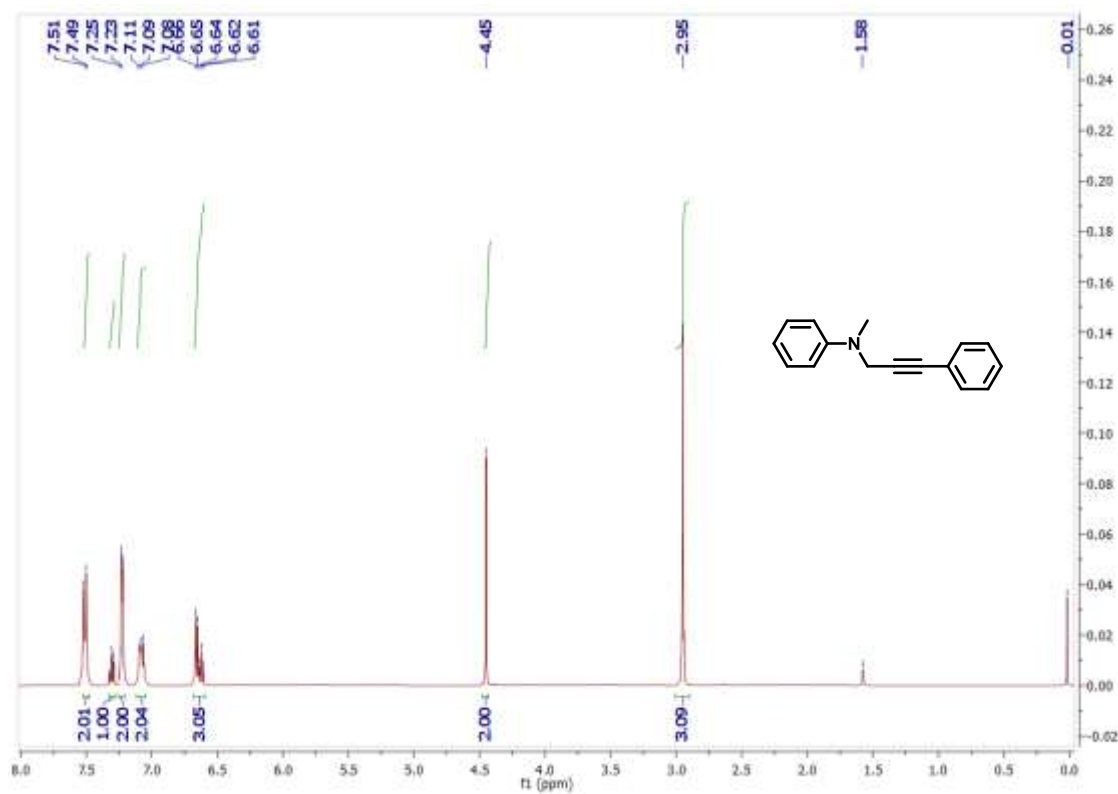


Fig. S48 ¹H NMR spectrum of derivative **9b** in CDCl₃

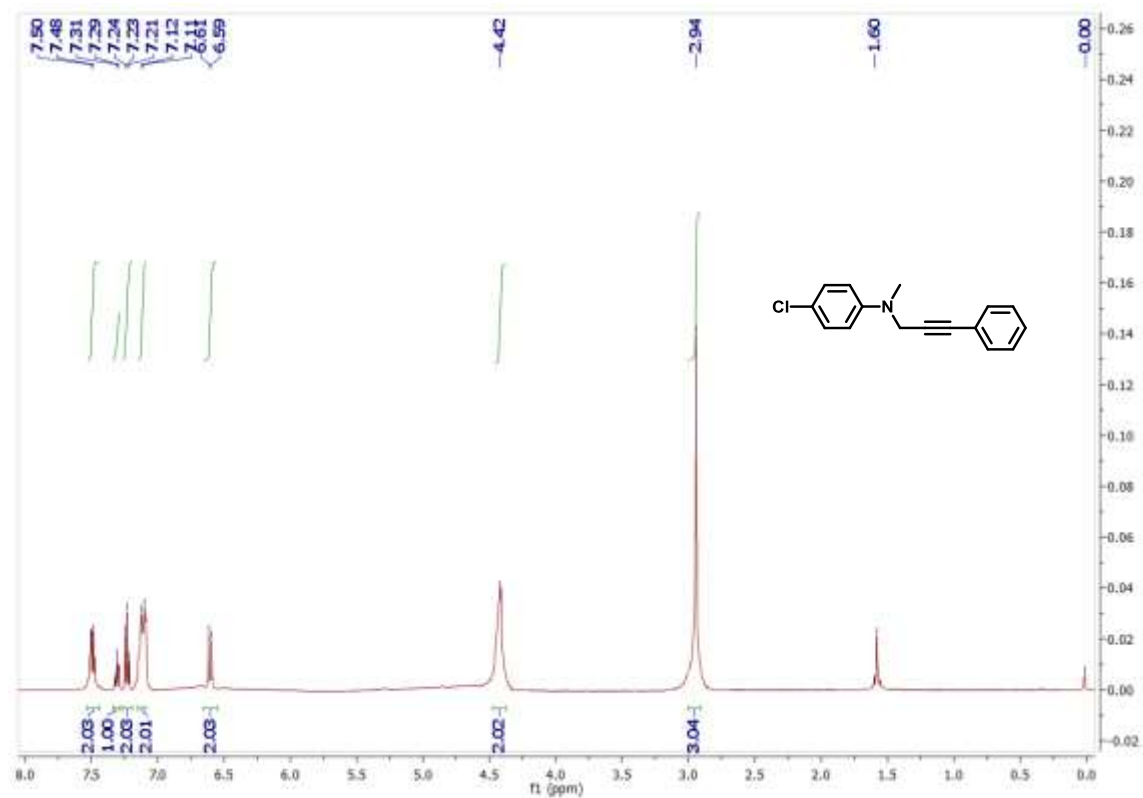


Fig. S49 ^1H NMR spectrum of derivative **9c** in CDCl_3

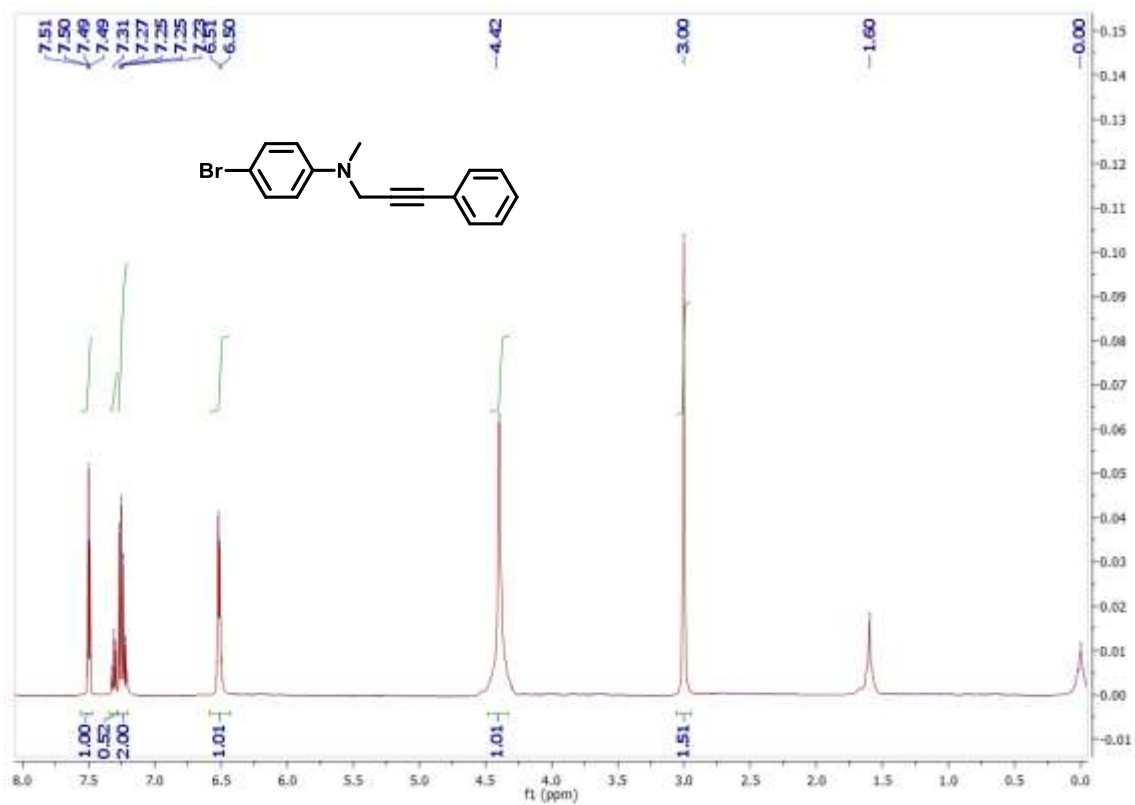


Fig. S50 ^1H NMR spectrum of derivative **9d** in CDCl_3

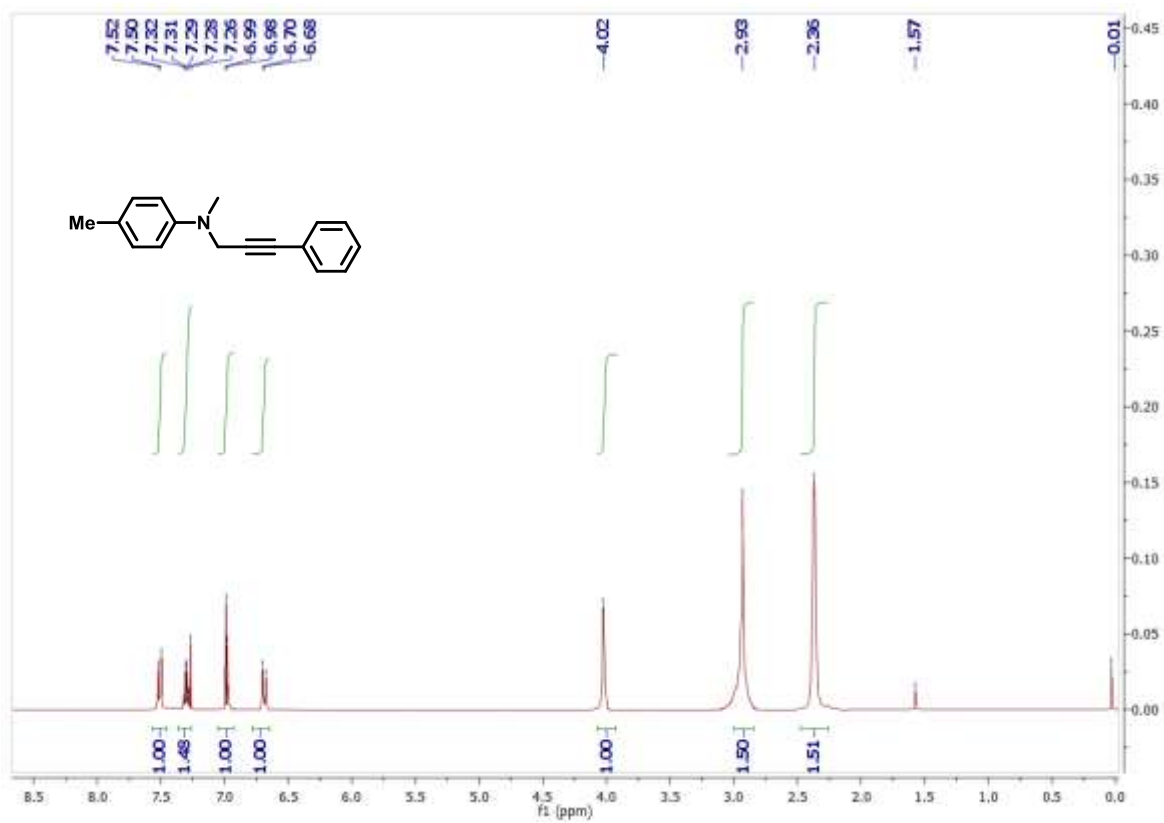


Fig. S51 ^1H NMR spectrum of derivative **9e** in CDCl_3

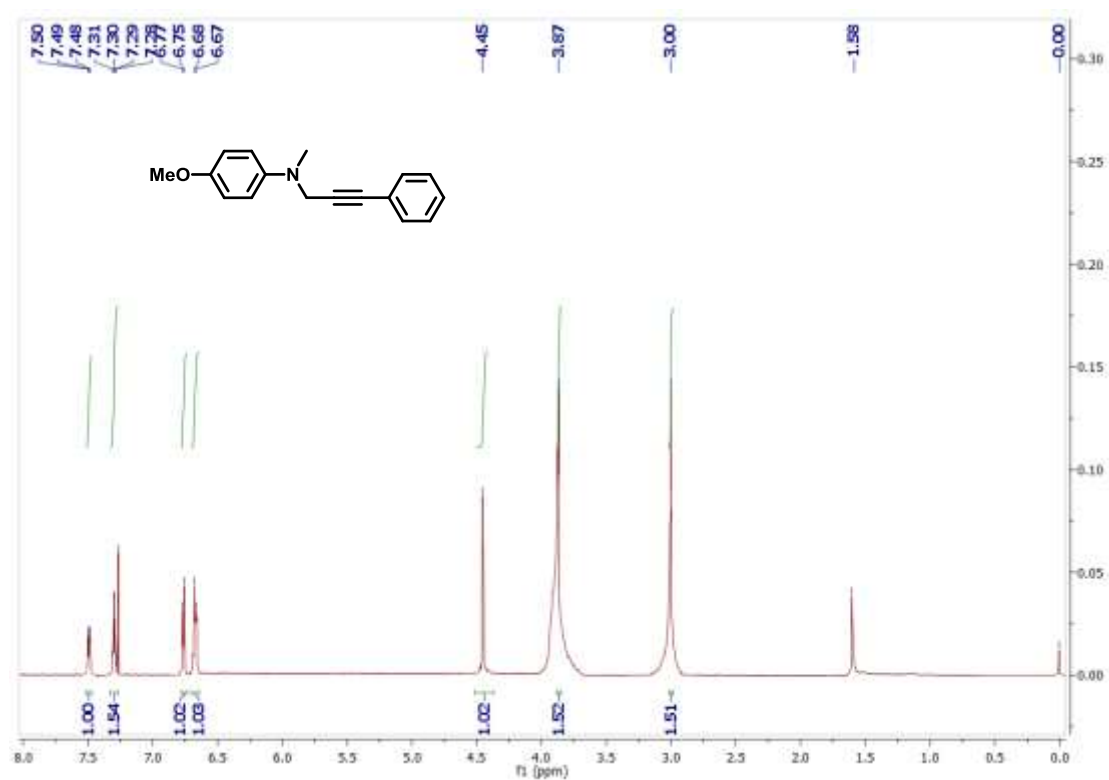


Fig. S52 ¹H NMR spectrum of derivative **11a** in CDCl₃

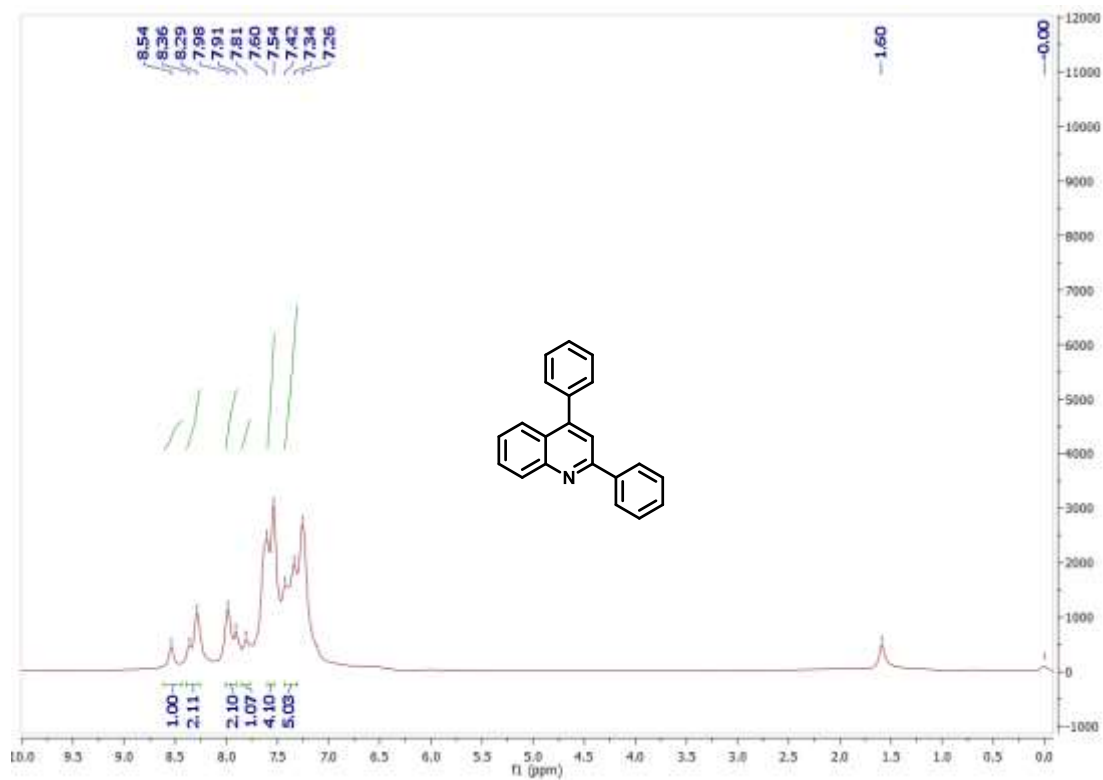


Fig. S53 ¹H NMR spectrum of derivative **11b** in CDCl₃

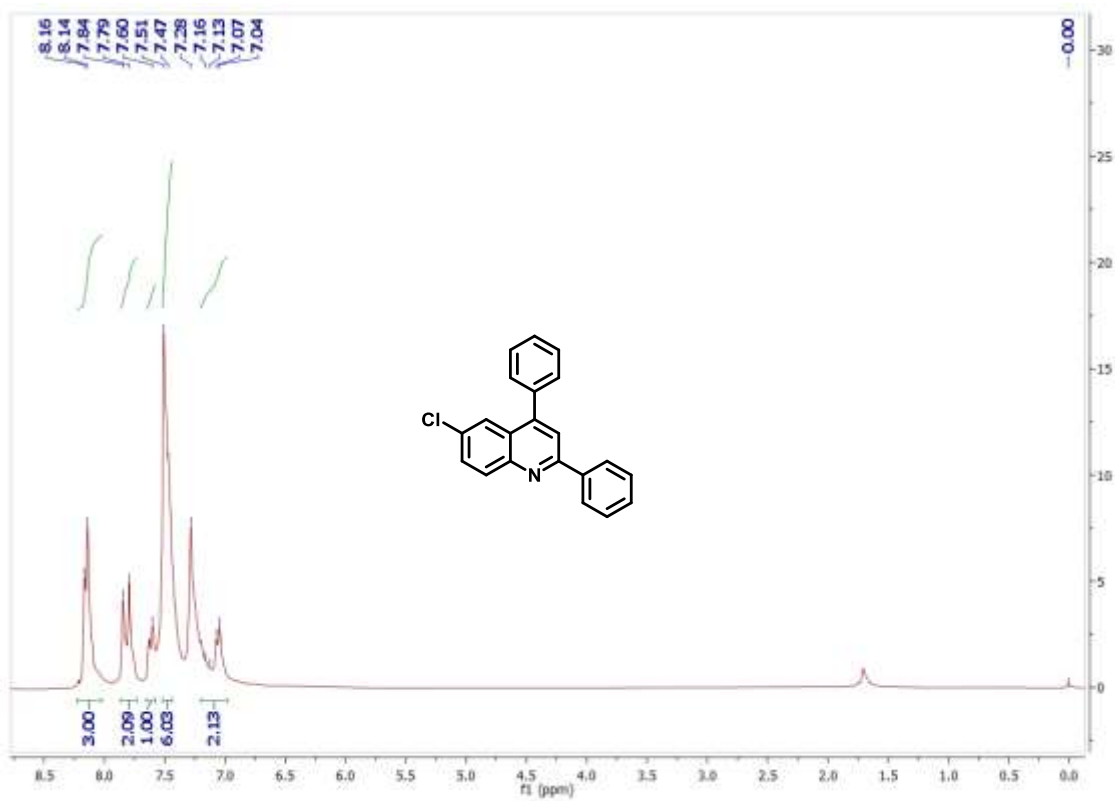


Fig. S54 ^1H NMR spectrum of derivative **11c** in CDCl_3

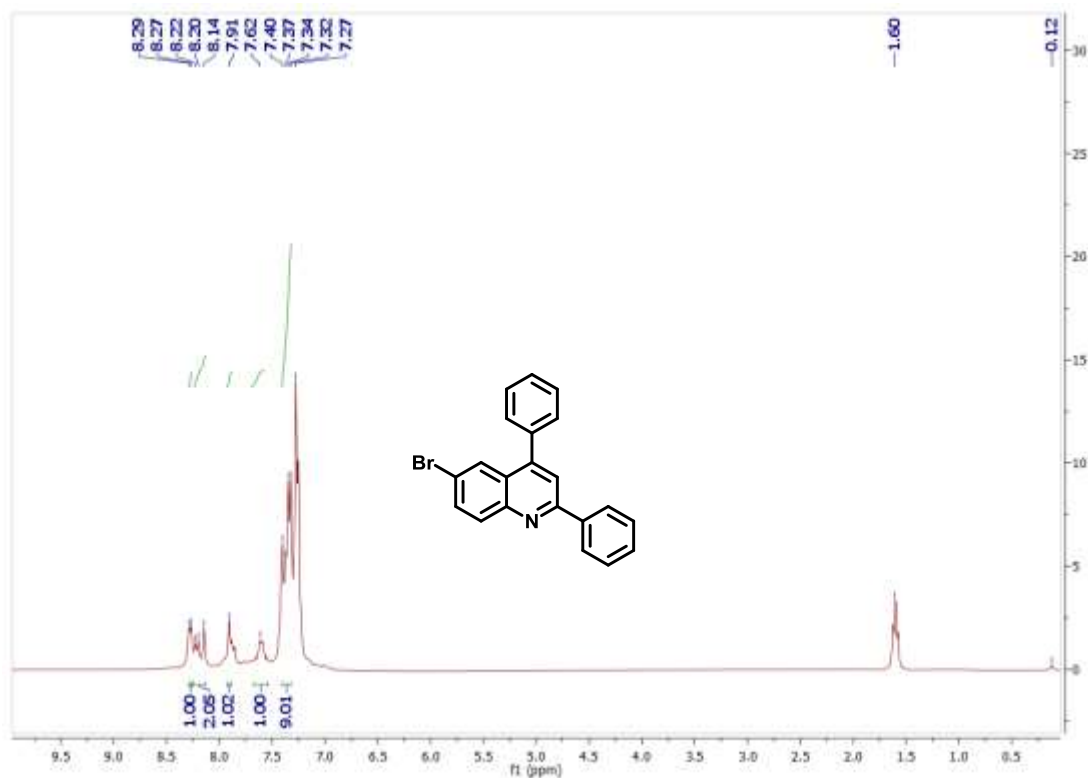


Fig. S55 ^1H NMR spectrum of derivative **11d** in CDCl_3

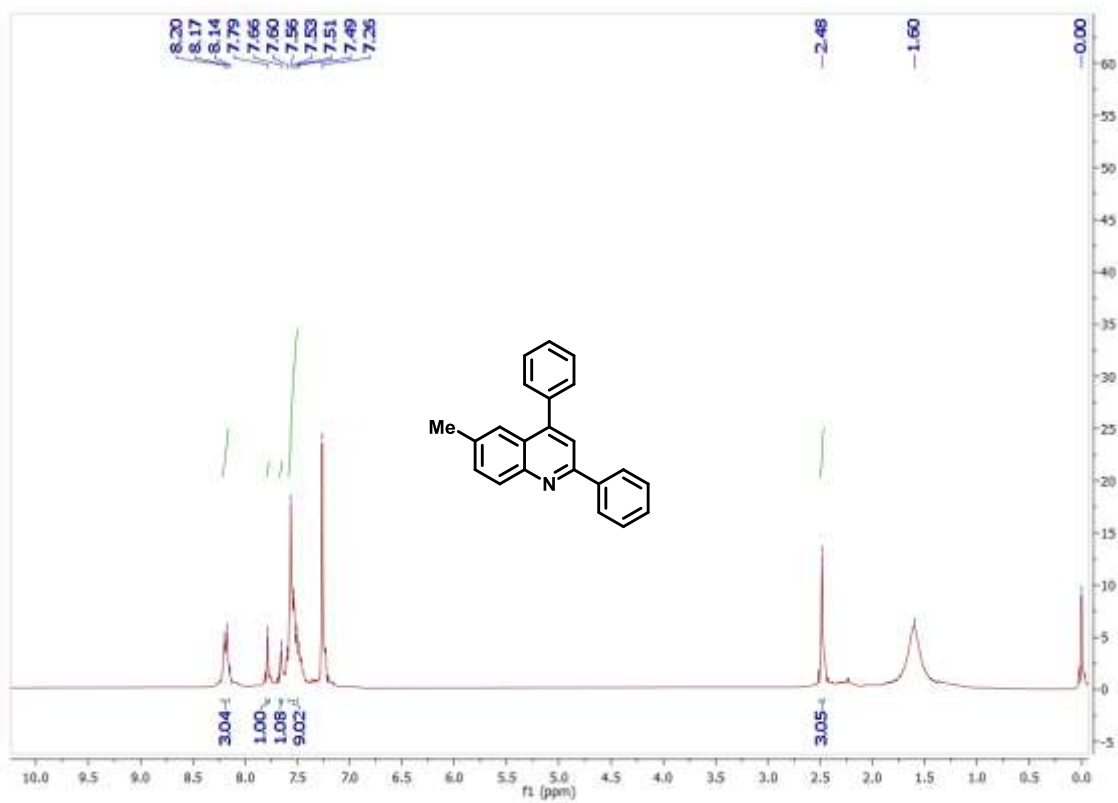


Fig. S56 ^1H NMR spectrum of derivative **11e** in CDCl_3

